C1

Immunolocalization of the zinc transporter hZTL1 at the apical membrane of human jejunum and Caco-2 cells

Ruth A. Cragg, Sion R. Phillips, John C. Mathers and Dianne Ford

School of Cell and Molecular Biosciences, University of Newcastle upon Tyne, Kings Road, Newcastle upon Tyne NE1 7RU, UK

We previously reported the cloning of an intestinal zinc transporter hZTL1 which, when expressed in human intestinal Caco-2 cells with a C-terminal Myc epitope tag, was located at the apical membrane (Cragg *et al.* 2002). Here, we confirm the localization of hZTL1 in Caco-2 cells and report the location of hZTL1 in sections of human jejunum using an hZTL1 antipeptide antibody.

Rabbit anti-hZTL1 antibody was raised against a synthetic peptide corresponding to amino acids 190–211 of hZTL1 (ILSSPSKRGQKGTLIGYSPEGT) and was affinity purified. Human jejunum was obtained from cadaver donors with appropriate ethics committee approval. Frozen sections (7 μm) were fixed for 30 min on ice with 4 % (w/v) paraformaldehyde in PBS. Caco-2 cells, grown for 14 days on polycarbonate filters, were fixed with 100 % methanol for 5 min at room temperature. Sections or cells were permeabilized in 0.1 % (v/v) Triton X-100 in PBS and incubated in blocking solution (5 % w/v BSA, 10 % (v/v) goat serum, 0.1 % Triton X-100 in PBS). After incubation overnight at 4°C with anti-hZTL1 antibody (1:100), slides were washed in PBS and samples were then incubated with FITC-conjugated goat anti-rabbit IgG (1:500) for 1 h at room temperature. Caco-2 cells were subsequently treated with propidium iodide to reveal nuclear staining or with a chromogenic alkaline phosphatase stain. Sections or filters were mounted in fluorescence mounting medium under a sealed coverslip and visualized using a Leica confocal microscope.

Specific FITC staining was localized at the apical membrane of human jejunum and was concentrated towards the villus tip. In Caco-2 cells, staining was observed exclusively at the apical membrane and co-localized with alkaline phosphatase activity. These data are consistent with the established location of hZTL1 in Caco-2 cells using the Myc-tagged construct (Cragg *et al.* 2002).

Comparison of the cDNA sequences of hZTL1 and ZnT5 (Kambe *et al.* 2002) reveals that they are splice variants of the same gene. The antibody used in the study reported here corresponds to a region common to both hZTL1 and ZnT5. We have previously reported that the ZnT5 variant, shown to localize to intracellular vesicles in pancreas (Kambe *et al.* 2002), is not detected in Caco-2 cells by RT-PCR (Russi *et al.* 2003). The absence of a vesicular staining pattern in either human intestine or Caco-2 cells reported here is consistent with the expression of only hZTL1 in intestine and adds to the evidence that hZTL1/ZnT5 splice variants are expressed in a tissue-specific manner.

Cragg RA *et al.* (2002). *J Biol Chem* **277**, 22789–22797.

Kambe *et al.* (2002). *J Biol Chem* **277**, 19049–19055.

Russi RM *et al.* (2003). *J Physiol* (**in Press**) *P*.

This work was supported by BBSRC grant 13D/11012

All procedures accord with current UK legislation and the use of human tissue was covered by ethics committee approval.

C2

Identification of the placental Cu oxidase as eleutherin, a hephaestin homologue

S. Dunford, H.S. Andersen, C. Fosset, C. Vulpe*, R. Danzeisen, L. Gambling and H.J. McArdle

*Rowett Research Institute, Bucksburn, Aberdeen, UK and *Department of Nutritional Sciences and Toxicology, University of California, Berkeley, CA, USA*

The mechanism of iron release from the placenta is not well understood. We have previously identified a copper oxidase that appears to be intimately involved in the process and have shown that it was regulated by copper and by iron levels in placental cells (BeWo) (Danzeisen *et al.* 2002). Recently, we identified sequences in the database with a high degree of homology to both hephaestin and serum ceruloplasmin (www.ncbi.nlm.nih.gov accession numbers XP-100543, and XP-146812). Here, we demonstrate, using reverse transcriptase–polymerase chain reaction (PCR), siRNA, Western blotting and real-time PCR, that this gene codes for the placental Cu oxidase.

BeWo cells were grown in Ham's F12 supplemented with 10 % fetal bovine serum with or without antibiotics as appropriate. Cells were grown to approximately 80 % confluence. For siRNA experiments, the cells were treated according to methods provided on the Ambion web site (www.ambion.com) and using templates designed according to the manufacturer's instructions (*Ambion Silencer^{TM} siRNA Construction Guide*). Cells were transfected with the siRNA using siPortAmine (Ambion) according to the manufacturer's instructions after optimisation for BeWo cells. Following transfection, cells were scraped and solubilised in running buffer before being separated on 7.5 % SDS–PAGE gels. Oxidase protein was visualised using anti-ceruloplasmin antibody (Danzesien *et al.* 2002). Real-time PCR was performed using the TaqMan system (Perkin Elmer).

As would be expected, the sequences showed a putative membrane-spanning sequence and multi-copper binding site. Reverse transcriptase–PCR reactions gave a single band of the predicted size, which, when sequenced, matched the gene in the data base. We tested the hypothesis that the mRNA coded for the oxidase protein by using siRNA followed by immunoblotting. Transfecting the cells with increasing concentrations of siRNA resulted in a dose-dependent decrease in oxidase protein. This is direct evidence that the gene codes for the placental oxidase.

We have previously shown that the oxidase protein and activity levels are regulated by copper and iron. Here, we demonstrate, using real time PCR, that mRNA levels are decreased by treatment with a copper chelator, but are not altered by iron chelators. We propose calling this member of the Cu oxidase family 'eleutherin' after Eleutheria, the sister of Hephaestos and the goddess of midwives.

Danzeisen R *et al.* (2002). *Am J Physiol* **282**, C472–478.

This work was funded by SEERAD, EUFPV, and the International Copper Association.

C3

PKG II-dependent inhibition of an Fe^{2+}-evoked electrogenic transport pathway by cGMP in human intestinal Caco-2 epithelia

Derek A. Scott*, Harry J. McArdle† and Gordon T.A. McEwan*

*Department of Biomedical Sciences, Institute of Medical Sciences, University of Aberdeen, Aberdeen AB25 2ZD and †Rowett Research Institute, Greenburn Road, Aberdeen AB21 9SB, UK

Apical exposure to Fe^{2+} stimulates a pH-dependent inward short circuit current (I_{SC}) in Caco-2 epithelia (Scott *et al.* 2002). This transport process is consistent with H^+-coupled apical entry of Fe^{2+} via DMT-1 (Gunshin *et al.* 1997). The present study set out to investigate intracellular regulation of Fe^{2+}-evoked electrogenic transport by cGMP.

I_{SC} determinations were made on voltage-clamped Caco-2 epithelia, grown on permeable supports (Anotec, Nunc). Cells were bathed with isotonic mannitol–Hepes buffer (37°C; pH 7.4). At the onset of the experiment, apical pH was adjusted to 6.0. Iron ascorbate (1:10 molar ratio) was applied apically. The cGMP analogue 8-Br cGMP (100 μM) was applied to the apical bathing medium for 20 min prior to Fe^{2+} exposure. In experiments investigating the effects of staurosporine (0.5 μM), The PKA inhibitor H-89 (50 μM) and the PKG II inhibitor Rp-8-pCPT-cGMPs (20 μM), these were applied 30 min prior to 8-Br cGMP.

Exposure to 8-Br cGMP inhibited Fe^{2+}-induced inward I_{SC} to levels not distinguishable from zero at all Fe^{2+} concentrations tested (25–1000 μM). Pre-incubation with staurosporine reversed cGMP-induced inhibition of Fe^{2+}-evoked I_{SC} and stimulated ($P < 0.05$, ANOVA) an additional inward I_{SC} (control $V_{max} = 1.06 \pm 0.05$ μA cm^{-2} (9); stauro + cGMP $V_{max} = 1.71 \pm 0.12$ μA cm^{-2} (5) (means ± S.E.M. (n)). Staurosporine alone stimulated the Fe^{2+}-induced I_{SC} with V_{max} rising ($P < 0.001$ *vs.* control) to 2.45 ± 0.40 μA cm^{-2} (4). Rp-8-pCPT-cGMPs also abolished the inhibitory action of 8-Br cGMP on Fe^{2+}-induced I_{SC} (control $V_{max} = 1.05 \pm 0.15$ μA cm^{-2} (4); Rp-8-pCPT-cGMPs + cGMP $V_{max} = 0.99 \pm 0.04$ μA cm^{-2} (4)). As with staurosporine, Rp-8-pCPT-cGMPs alone stimulated the Fe^{2+}-induced I_{SC}, V_{max} rising ($P < 0.01$) to 1.99 ± 0.21 μA cm^{-2} (4). H89 had no effect on the actions of 8Br-cGMP or on the Fe^{2+}-evoked I_{SC}.

These data identify an intracellular regulatory mechanism for an Fe^{2+}-induced electrogenic transport pathway in Caco-2 epithelia. Regulation by cGMP was inhibitory and was dependent upon PKG II with no discernible involvement of PKA. The stimulatory actions of both staurosporine and Rp-8-pCPT-cGMPs when applied alone suggest that there was baseline inhibitory PKG II activity in these cells. To our knowledge, this is the first reported involvement of cGMP/PKG II-dependent regulation of an Fe^{2+}-evoked transport pathway.

Gunshin H *et al.* (1997). *Nature* **388**, 482–488.

Scott DA *et al.* (2002). *J Physiol* **539.P**, 19*P*.

D.A.S. was supported by a BBSRC PhD studentship.

C5

Iron and zinc differentially regulate Fe^{2+}- and Zn^{2+}-induced electrogenic transport pathways in human intestinal Caco-2 epithelia

Derek A. Scott*, Harry J. McArdle† and Gordon T.A. McEwan*

*Department of Biomedical Sciences, Institute of Medical Sciences, University of Aberdeen, Aberdeen AB25 2ZD and †Rowett Research Institute, Greenburn Road, Aberdeen AB21 9SB, UK

We have previously reported on the stimulation of pH-dependent electrogenic transport pathways following exposure to apical Fe^{2+} and Zn^{2+} in Caco-2 epithelia (Scott *et al.* 2002). The present study set out to establish the effects of chronic Fe^{2+} and Zn^{2+} loading and Fe^{2+} depletion on these transport routes.

Short circuit current (I_{SC}) determinations were made on voltage-clamped Caco-2 epithelia, grown on permeable supports (Anotec, Nunc). Cells were bathed with isotonic mannitol/Hepes buffer (37°C; pH 7.4). At the onset of the experiment, apical pH was adjusted to 6.0. Iron ascorbate (1:10 molar ratio) or zinc histidine (1:5) was applied apically. For Fe^{2+} or Zn^{2+} loading, 100 μM of either Fe^{2+} or Zn^{2+} was added to culture medium for 24 h prior to experimentation. For Fe^{2+} depletion, 100 μM desferrioxamine was added to culture medium 40 h prior to experimentation. All conditions were accompanied by time-matched vehicle controls from the same cell batch.

Under Fe^{2+}-depleted conditions, the Fe^{2+}-induced inward I_{SC} was enhanced with V_{max} rising significantly ($P < 0.01$, Student's unpaired t test, means ± S.E.M. (n)) from 0.97 ± 0.12 (5) to 2.04 ± 0.18 μA cm^{-2} (5). In contrast, Fe^{2+} depletion resulted in a reduction in the Zn^{2+}-induced I_{SC}, V_{max} falling ($P < 0.02$) from 1.25 ± 0.07 (4) to 0.95 ± 0.05 μA cm^{-2} (4). Fe^{2+} loading reduced the Fe^{2+}-evoked I_{SC} at all Fe^{2+} concentrations tested (1–500 μM; $P < 0.05$–0.001) with transport failing to display saturation. However, Fe^{2+} loading had no effect on the Zn^{2+}-induced I_{SC}. Zn^{2+} loading enhanced the Fe^{2+}-induced I_{SC} by over 300 % with V_{max} rising ($P < 0.001$) from 0.89 ± 0.13 (5) to 3.4 ± 0.19 μA cm^{-2}. In striking contrast, Zn^{2+} loading reversed ($P < 0.001$) the inward I_{SC} observed under control conditions ($V_{max} = 0.77 \pm 0.12$ μA cm^{-2} (5)) to a significant ($P < 0.05$) saturable outward I_{SC} with a V_{max} of 1.11 ± 0.27 μA cm^{-2}.

These data demonstrate that Fe^{2+} and Zn^{2+}-evoked electrogenic transport pathways are differentially affected by altering the exposure levels to these metals. This provides evidence that some or all of the transporters involved in these pathways are regulated by both Fe^{2+} and Zn^{2+}. The present data are consistent with previously published data demonstrating regulation of DMT-1 expression by Fe^{2+} and Zn^{2+} (Yamaji *et al.* 2001). However, it does not support the view that Fe^{2+} and Zn^{2+} are transported by a common pathway.

Scott DA *et al.* (2002). *J Physiol* **539.P**, 19*P*.

Yamaji S *et al.* (2001). *FEBS Lett* **507**, 137–141.

D.A.S. was supported by a BBSRC PhD studentship.

C6

Expression of divalent metal transporter DMT1 is coordinated during development and spermatogenesis in rat testis

K.P. Griffin, D.T. Ward, S. McLarnon, G.S. Stewart, I.D. Morris* and C.P. Smith

*School of Biological Sciences, University of Manchester, Oxford Road, Manchester M13 9PT and *Hull York Medical School, University of York, Heslington, York YO10 5DD, UK*

Iron is essential to fertility as it is required for germ cell division, differentiation and metabolism. DMT1 is expressed in the apical membranes of duodenal enterocytes and is responsible for the non-transferrin-mediated absorption of dietary iron. DMT1 is also expressed in vesicular membranes and participates in transferrin-mediated iron acquisition by cells. It is highly expressed in the kidney and is thought to play a role in renal iron handling. The aim of this study was to determine the pattern of DMT1 expression in the rat testis.

Peroxidase immunohistochemistry using an affinity-purified anti-DMT1 polyclonal antibody targeted to recognise all DMT1 isoforms (Ferguson *et al.* 2001) was used to study the cellular distribution of DMT1. Western analysis was used to quantify the levels of DMT1 in the testis of humanely killed 5-, 15-, 25-, 35-day-old and adult rats.

DMT1 immunoreactive species were detected throughout development in the seminiferous tubules but not in the interstitium. In the 5- and 15-day-old rats, immunostaining was equally widespread throughout each tubule and could be localised to the cytoplasm of the Sertoli cells. This was the case in the 25- and 35-day-old animals but more punctate areas could be detected.

In the adult rat immunostaining was specific to each of the 14 stages of the cycle of the seminiferous epithelium and as a result tubules appeared heterogeneous, unlike in the immature rat. Staining could be localised to the nuclei and cytoplasm of both Sertoli and germ cells. The most intense immunoreactivity appeared at Stages VII and VIII and could be attributed mainly to the deep staining of the mature spermatozoa, suggesting that these cells have a high requirement for iron as they prepare to leave the seminiferous tubules.

Western analysis detected an immunoreactive protein band of around 60 kDa in the membrane fractions at all ages tested. At 15, 25 and 35 days and in the adult rat a second higher weight band was detected of around 70 kDa, revealing expression of a different isoform at these ages. Deglycosylation experiments with *N*-glycosidase showed that the major DMT1 isoform present (55 kDa) was different from that in the kidney (50 kDa).

The expression profile of DMT1 in the development of the rat testis was found to be cell specific and highly co-ordinated to the spermatogenic cycle. This suggests an important role for DMT1 in spermatogenesis and implies that the germ cells have a need for a precisely timed supply of iron. This stage-specific nature of expression means that DMT1 plays a central role in male fertility. This may be applicable when considering conditions of abnormal iron regulation.

Ferguson *et al.* (2001). *Am J Physiol Renal Physiol* **280**, F803–814.

This work was funded by the BBSRC, The Royal Society and The Wellcome Trust

All procedures accord with current UK legislation.

C7

Site-directed mutagenesis investigations of the substrate-binding site of the rabbit proton-coupled peptide transporter PepT1 expressed in *Xenopus* oocytes

D. Meredith

Department of Human Anatomy and Genetics, South Parks Road, Oxford OX1 3QX, UK

The proton-coupled di- and tri-peptide transporter isoform PepT1 has an exceptionally wide substrate range, leading to interest in understanding the substrate-binding site (see Meredith & Boyd, 2000 for a review). Here we report the results of site-directed mutagenesis experiments to test whether particular highly conserved residues play a predictable role in PepT1 function, with the aim of further refining our substrate template model (Bailey *et al.* 2000).

Selected rabbit PepT1 residues were mutated using a PCR-based protocol (Quikchange, Stratagene) and confirmed by DNA sequencing. Uptake experiments into PepT1-expressing *Xenopus laevis* oocytes were performed as previously described (Meredith *et al.* 2000). Data are means ± S.E.M.; $n = 5$ oocytes.

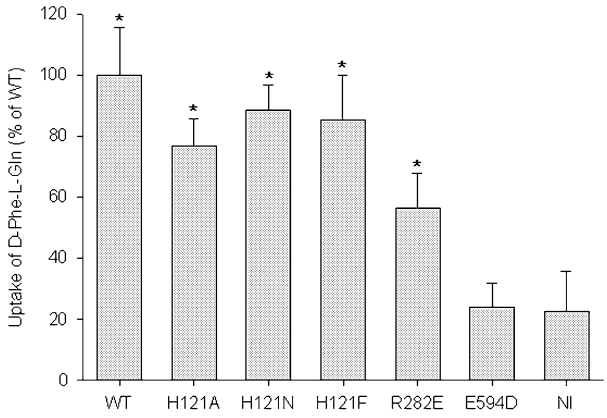

Figure 1. Uptake of 0.42 μM ^{3}H-D-Phe-L-Gln into *Xenopus* oocytes expressing wild-type (WT) or mutated PepT1. No correction has been made for protein expression level. *$P < 0.001$ compared to control (NI) (Student's unpaired t test).

His_{121} has been proposed as playing a role in the binding of the side chain of the second residue in a dipeptide, with the protonated form ($HisH^+$) donating a proton to the COO^- of acidic residues (Chen *et al.* 2000). The H121A, H121N and H121F PepT1 mutations were virtually unaffected, as might be predicted for uptake of a neutral substrate (Fig, 1). Arg_{282} has been predicted from computer modelling to be involved in regulating translocation of substrates through PepT1, although the V_{max} of R282A-hPepT1 was only reduced 15 % (Bolger *et al.* 1998). Indeed, as can be seen in Fig. 1, even after swapping the wild-type positively charged residue for a negative glutamate, R282E-PepT1 could still perform transport. Finally, Glu_{594} has been proposed as the binding site for the amino terminus NH_3^+ group of substrates (Meredith *et al.* 2000). Conservative substitution of this residue for negatively charged Asp (E594D, Fig. 1) abolished uptake, suggesting that simply the presence of a negatively charged amino acid residue at this point in the sequence is insufficient for functional protein.

These preliminary results confirm and extend existing studies implicating His_{121} and Glu_{594} in the functioning of the PepT1 transport protein. The role of Arg_{282} is currently less clear.

Further studies will be required to elucidate the full roles of these residues in PepT1 in substrate binding and translocation.

Bailey PD *et al.* (2000). *Ang Chemie Int Ed* **39**, 505–508.
Bolger MB *et al.* (1998). *J Pharm Sci* **87**, 1286–1291.
Chen XZ *et al.* (2000). *Biochem Biophys Res Comm* **272**, 726–730.
Meredith D & Boyd CAR (2000). *Cell Mol Life Sci* **57**, 754–778.
Meredith D *et al.* (2000). *Eur J Biochem* **267**, 3723–3728.

This work is generously funded by the Wellcome Trust.

All procedures accord with current UK legislation.

C8

Altered affinity for cationic amino acid transport through system y$^+$L following forskolin treatment of cultured BeWo cells

R. Laynes, Y. Kudo, C.A.R. Boyd and R. Devés*

*Department of Human Anatomy and Genetics, South Parks Road, Oxford OX1 3QX, UK and *Department of Physiology and Biophysics, University of Chile, Santiago 7, Chile*

The human placental trophoblast tumour cell line BeWo can be induced to syncytialise following forskolin. During a microarray expression study of forskolin-regulated genes in these cells (Kudo *et al.* 2002) we noted striking and reciprocal changes (up-regulation, down-regulation respectively) in the levels of mRNA encoding the amino acid transporters y$^+$LAT-2 and y$^+$LAT-1. These membrane proteins are the two isoforms of the catalytic light chains of the y$^+$L amino acid transport system. We have therefore studied transport through system y$^+$L in these cells with and without 36 h pre-treatment with forskolin to see whether there are alterations in transport function associated with the altered gene expression.

Table 1. y$^+$L mediated lysine flux (V_i/V_o)

	Control	+Forskolin
+Lys (10 μM)	0.60	0.42
+Lys (100 μM)	0.26	0.14

Table 2. y$^+$L mediated arginine flux (V_i/V_o)

	Control	+Forskolin
+Arg (10 μM)	0.32	0.21
+Arg (100 μM)	0.13	0.05

Because we were interested in determining both affinity and velocity for different known system y$^+$L substrates we used a mixture of two cationic amino acids (lysine, arginine) as substrates, each at low concentration (1 μM) with a modified protocol for determining amino acid influx (Kudo & Boyd, 2002) under initial rate conditions (3 min, 37 °C) using double label (L-[^{14}C]arginine, L-[^{3}H]lysine). We observe high affinity inhibition of more than 95 % of total cationic amino acid influx by 10 mM glutamine in both control and forskolin (100 μM) treated cells (K_i is 90 μM in control and 30 μM in treated cells). Since in the absence of sodium (choline substituting), total cationic amino acid transport fluxes are substantially unaltered whereas the affinity for inhibition by glutamine is very markedly reduced, we conclude that at the low substrate concentration used in this study virtually all of the flux of cationic amino acids into these cells is through system y$^+$L (in contrast to the conclusion of Way *et al.* 1998). We find (Tables 1 and 2) that cells treated with forskolin have a higher affinity for inhibition (V_i) of system y$^+$L by either amino acid than do control (vehicle-only) cells. Taken together with the array data this indicates that, in mammalian cells at 37 °C, y$^+$LAT1 has a lower affinity than does y$^+$LAT2 for cationic amino acids (compatible with findings made in the *Xenopus* oocyte expression system at room temperature; Pfeiffer *et al.* 1999; Broer *et al.* 2000). A novel behaviour of system y$^+$L in these cells is the finding that arginine is a better inhibitor of arginine flux than of lysine flux. Lysine on the other hand appears to have the same effect on both fluxes. This may be explained if there are different transport activities for each amino acid.

Broer A *et al.* (2000). *Biochem J* **349**, 787–795.
Kudo Y & Boyd CAR(2002). *Placenta* **23**, 536–541.
Kudo Y *et al.* (2002). *J Physiol* **539.P**, 127*P*.
Pfeiffer R *et al.* (1999). *EMBO J* **18**, 49–57.
Way BA *et al.* (1998). *Placenta* **19**, 323–8.

We are grateful to the Wellcome Trust for financial support.

C9

Lithium stimulates glucose transport in rat skeletal muscle cells by a mechanism that is independent of glycogen synthase kinase-3: the potential role of p38 MAP kinase

K. MacAulay, E. Hajduch, A.S. Blair, M.P. Coghlan*, S.A Smith* and Harinder S. Hundal

*Division of Molecular Physiology, University of Dundee, Dundee, DD1 5EH and *GlaxoSmithKline, Coldharbour Road, The Pinnacles, Harlow, Essex CM19 5AD, UK*

Glycogen synthase kinase 3 (GSK3) is a serine/threonine kinase that has been implicated in the regulation of diverse physiological responses, including glycogen metabolism (Frame & Cohen, 2001). GSK3 is inhibited by insulin and lithium and, like the hormone, Li has been shown to stimulate glucose transport and induce activation of glycogen synthase (GS) (Chen *et al.* 1998; Orena *et al.* 2000), leading to the suggestion that GSK3 inactivation may be of importance for the hormonal stimulation of glucose transport. In the present study we have used Li and SB-415286, a maleimide derivative that selectively inhibits GSK3 (Coghlan *et al.* 2000), to test this proposition in rat L6 myotubes.

Insulin stimulated glucose transport by ~2-fold and induced inactivation of GSK3 by ~50 %. This inhibition in GSK3 led to an increase in GS activity by ~4.2-fold. Like insulin, Li and SB-415286 induced a significant reduction in GSK3 activity (by 73 % and 97 %, respectively) and caused a corresponding stimulation in GS, which was comparable to or greater than that elicited by insulin. L6 cells exposed to Li for 1 h induced a dose-dependent increase in glucose transport which was stimulated maximally to over 2-fold by 50 mM Li. Replacing Li with an equivalent concentration of sucrose did not mimic this effect suggesting that the response was not due to osmotic shock. In contrast, SB-415286 had no detectable effect on glucose transport. The Li-induced increase in glucose uptake was not sensitive to inhibitors of phosphoinositide 3-kinase, the classical mitogen-activated protein (MAP) kinase pathway or the mammalian target of rapamycin, but was suppressed completely by SB-203580, a p38 MAP kinase inhibitor. Li also induced a dose-dependent activation of p38 MAP kinase in L6 cells in a SB-203580 sensitive manner.

Our findings support a role for GSK3 in the chemical inactivation of GS which is sufficient to elicit a decrease in GS activity. We propose, based on the differential effects of Li and SB-415286, that GSK3 is unlikely to contribute towards the hormonal regulation of glucose transport in insulin target

tissues, as previously suggested (Orena *et al.* 2000; Chen *et al.* 1998). Instead, our data indicate that this stimulation arises through activation of p38 MAP kinase.

Chen X *et al.* (1998). *Am J Physiol* **275**, E272–277.
Coghlan MP *et al.* (2000). *Chem Biol* **24**, 1–11.
Frame & Cohen (2001). *Biochem J* **359**, 1–16.
Orena S *et al.* (2000). *J Biol Chem* **275**, 15765–15772.

This work was supported by the MRC, BBSRC, Diabetes UK and GlaxoSmithKline.

C10

Diethylpyrocarbonate abolishes pH sensitivity of System A (SAT2) amino acid transporter

F.E. Baird, H.S. Hundal and P.M. Taylor

Faculty of Life Sciences, University of Dundee, Dundee DD1 5EH, UK

The Na^+-coupled System A amino acid transporters (SAT1–3) exhibit marked pH sensitivity, with influx depressed as external pH is lowered within the physiological range (Yao *et al.* 2000; Chaudhry *et al.* 2002); this may have important physiological implications for tissue amino acid and protein metabolism. (Bevington *et al.* 2002). We have investigated the possibility that this pH sensitivity relates to functionality of histidine residues within the transporter (SAT2) structure.

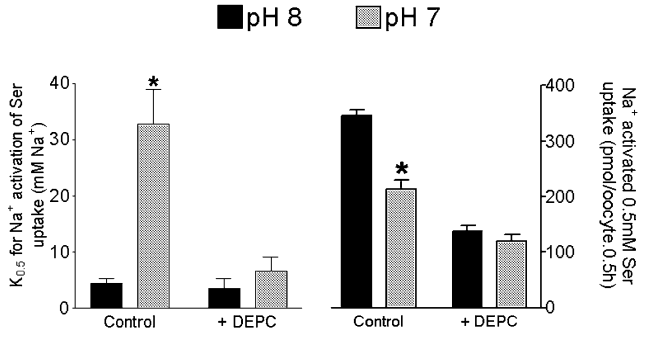

Figure 1. Effects of DEPC (2 mM, 10 min) on serine uptake in SAT2-expressing *Xenopus* oocytes. Values estimated from measurements at 6 different [NaCl] each using 8–11 oocytes. * $P < 0.05$ from pH 8 value; unpaired *t* test.

Rat SAT2 (Yao *et al.* 2000) was studied by overexpression in *Xenopus laevis* oocytes. SAT2 cRNA (50 ng) was injected into oocytes and experiments were performed 2–3 days later. L-[^{3}H]Serine (0.5 mM) influx through SAT2 was measured at pH 7 and 8 with NaCl concentrations of 0−100 mM (TMACl added to maintain osmolarity). Values shown are means ± S.E.M.

Pre-treatment of SAT2-expressing oocytes with the histidine-modifying reagent diethylpyrocarbonate (DEPC) resulted in substantial reduction of serine transport activity (2 mM DEPC for 10 min produced maximal effect of 71 ± 5 % inhibition at pH 8; $n = 8$ expts) and loss of pH sensitivity over the pH range studied (Fig 1, right panel). DEPC treatment also blocks an increase in $K_{0.5}$ for Na^+ activation of 0.5 mM serine transport seen on switching from pH 8 to 7 (Fig. 1, left panel). Na^+ was not required for DEPC to inhibit transporter activity but the SAT2 substrate serine (5 mM) offered partial (~50 %) protection from the inactivating effects of DEPC. DEPC treatment abolishes pH sensitivity in the $K_{0.5}$ for Na^+ activation of SAT2 without significantly affecting the value at pH 8. This is consistent with DEPC acting to alleviate an inhibitory allosteric effect of H^+ on Na^+ binding (Albers *et al.* 2001), rather than reduce competition between Na^+ and H^+ for a common binding site (Chaudhry *et al.* 2002). DEPC pre-treatment appears to reduce the rate of substrate translocation through SAT2, although the inability of DEPC to completely block transport suggests that its site of action is not directly at an essential substrate binding site. We suggest that DEPC binds to histidine residue(s) in the SAT2 protein at (or near) a putative H^+ modifier site which may be in close proximity to the amino acid binding site (noting protection by serine).

Albers A *et al.* (2001). *Pflugers Arch* **443**, 92–101.
Bevington A *et al.* (2002). *Eur J Clin Invest* **32**, 590–602.
Chaudhry FA *et al.* (2002). *J Neurosci* **22**, 62–72.
Yao D *et al.* (2000). *J Biol Chem* **275**, 22790–7.

We thank Dr J.D. Erickson (Louisiana State University) for rat SAT2 cDNA. This work was funded by MRC.

C17

Acute and chronic effects of hydrocortisone on Na^+/H^+ exchanger activity in human renal proximal tubule cells

Brian J. Harvey and Cathy Halligan

Molecular Medicine, Royal College of Surgeons in Ireland, Smurfit Building, Beaumont Hospital, Dublin 9, Ireland

Glucocorticoids are reported to have stimulatory effects on renal proximal tubule Na^+/H^+ exchanger activity and on the expression of the NHE3 isoform. Here we have examined using spectrofluorescence microscopy, the effects of both acute and chronic exposure to hydrocortisone on luminal Na^+/H^+ exchanger activity in monolayers of primary cultured human proximal tubule (HPT) cells loaded with the pH-sensitive dye BCECF.

The cells were acid-loaded using the NH_4Cl pulse method under sodium-free conditions and Na^+/H^+ exchanger activity was measured as the initial slope of pH_i recovery (ΔpH_i units per min, means ± S.E.M., Student's paired *t* test) following the introduction of Na^+ to the luminal bath. Chronic exposure of HPT cells to hydrocortisone (10 nM for 90 min) increased the rate of Na^+-dependent pH_i recovery twofold when compared to untreated controls (control $\Delta pH_i = 0.10 \pm 0.02$, chronic hydrocortisone $\Delta pH_i = 0.23 \pm 0.03$, $n = 6$, $P \leqslant 0.001$). Acute (seconds) exposure to hydrocortisone produced an inhibition of NHE activity. Under these conditions, when hydrocortisone was introduced into the luminal bath with sodium, the pH_i recovery rate was reduced to 13 % of control (control $\Delta pH_i = 0.11 \pm 0.02$, acute hydrocortisone $\Delta pH_i = 0.013 \pm 0.012$, $n = 6$, $P \leqslant 0.005$). Pre-incubation of HPT cells for 10 min with the PKC inhibitor chelerythrine chloride (1 μM) had no effect on the stimulation of NHE after chronic exposure to hydrocortisone but did block the acute inhibition of NHE. On the contrary, preincubation of the cells for 20 min with the PKA inhibitor (RP)-cAMP (200 μM) inhibited the chronic stimulation of NHE but had no effect on the acute inhibition of NHE.

We conclude that chronic activation of NHE by hydrocortisone occurs via a PKA-dependent signalling pathway whereas acute inhibition of NHE is via PKC.

This work was funded by the Health Research Board of Ireland

All procedures accord with current National and local guidelines and the Declaration of Helskinki.

C18

Potent stimulation and inhibition of the human CFTR Cl^- channel by the fluorescein derivative Bengal Rose B

Z. Cai and D.N. Sheppard

Department of Physiology, University of Bristol, Bristol BS8 1TD, UK

The fluorescein derivative phloxine B (4,5,6,7-tetrachloro-2′,4′,5′,7′-tetrabromofluorescein) is a potent modulator of the cystic fibrosis transmembrane conductance regulator (CFTR) Cl^- channel. Low micromolar concentrations of phloxine B stimulate CFTR Cl^- currents, whereas higher concentrations of the drug inhibit CFTR (Bachmann *et al.* 2000; Cai & Sheppard, 2002). To understand better the structure–activity relationship of fluorescein derivatives, we studied Bengal Rose B (4,5,6,7-tetrachloro-2′,4′,5′,7′-tetraiodofluorescein), an agent with a chemical structure closely related to that of phloxine B.

The patch-clamp technique was used to investigate CFTR Cl^- channels in excised inside-out membrane patches from C127 cells stably expressing wild-type human CFTR (Cai & Sheppard, 2002). The pipette (external) solution contained 10 mM Cl^-, whereas the bath (internal) solution contained 147 mM Cl^-, PKA (75 nM) and ATP (0.3 mM) at 37 °C; voltage was −50 mV. Following the activation of CFTR Cl^- currents by cAMP-dependent phosphorylation, drugs were added to the intracellular solution. Nanomolar concentrations of Bengal Rose B (0.1–1 μM) stimulated CFTR Cl^- currents, whereas low micromolar concentrations of the drug (2–10 μM) inhibited CFTR. Bengal Rose B (0.1 μM) increased open probability (P_o) from 0.31 ± 0.06 to 0.40 ± 0.08 (means ± S.E.M., $n = 5$, $P < 0.05$, Student's paired t test), but caused a small, but significant decrease in current amplitude (i; $P < 0.05$). To determine how Bengal Rose B increased P_o, we investigated the drug's effects on gating kinetics using the QuB software suite (Cai & Sheppard, 2002). Bengal Rose B (0.1 μM) increased P_o by greatly prolonging mean burst duration (MBD) (control MBD = 116 ± 8 ms; Bengal Rose B MBD = 232 ± 30 ms; $n = 4$; $P < 0.05$) without significantly altering the inter-burst interval (IBI) (control IBI = 219 ± 19 ms; Bengal Rose B IBI = 307 ± 37 ms; $n = 4$; $P > 0.05$). However, the characteristics of channel block by Bengal Rose B differed from those of phloxine B. Inhibition of CFTR by phloxine is time independent. In contrast, during constant exposure to the drug, Bengal Rose B (2–10 μM) caused a progressive decrease of i until channel activity completely disappeared ($n = 10$).

We interpret these data to suggest that (i) Bengal Rose B interacts directly with CFTR at multiple sites to modulate channel activity; (ii) Bengal Rose B might stimulate CFTR by a similar mechanism to that of phloxine B; (iii) by modifying the residues at positions 2′,4′,5′,7′ of fluorescein, potent modulators of CFTR might be developed.

Bachmann A *et al.* (2000). *Br J Pharmacol* **131**, 433–440.

Cai Z & Sheppard DN (2002). *J Biol Chem* **277**, 19546–19553.

This work was supported by the CF Trust and NKRF.

C19

The Ca^{2+}-activated Cl^- conductance in mouse inner medullary collecting duct (mIMCD-K2) cells

S.H. Boese*, N.L. Simmon† and M.A. Gray†

**Zoophysiology, Institute for Biochemistry & Biology, University Potsdam, Lennestr. 7a, D-14471, Germany and †School of Cell & Molecular Biosciences, University Medical School, Framlington Place, Newcastle upon Tyne NE2 4HH, UK*

Mouse renal inner medullary collecting duct cells (mIMCD-K2 cell-line) possess a Ca^{2+}-activated Cl^- conductance (CaCC) which participates in transepithelial Cl^- secretion (Boese *et al.* 2000). We have now used whole cell patch clamp recordings to determine the dependence of CaCC upon intracellular $[Ca^{2+}]_i$ and noise analysis to estimate the conductance of the channel.

At 0.01 μM $[Ca^{2+}]_i$ only leakage currents were detected; at 0.1 μM $[Ca^{2+}]_i$ cell currents were very small. Only a slow outward relaxation was observed in response to the largest positive voltage (+80 mV) jump in some experiments whereas in others only leakage currents were seen. At 0.5 μM $[Ca^{2+}]_i$ relaxations of large amplitude were obtained. At 1.0 μM $[Ca^{2+}]_i$ and above, currents were large, but current relaxations were of small amplitude or not present, indicating that the channels were approaching full activation at all potentials tested. Fitting the $[Ca^{2+}]_i$ dependence of CaCC with a sigmoidal Hill equation gave EC_{50} values of 650.5 ± 31.4 nM (mean ± S.E.M. at −80 mV) and 306.1 ± 44.6 nM (at +80 mV) with Hill coefficients of 3.0 ± 0.3 and 1.7 ± 0.4, respectively. Diversity in Ca^{2+}-activated Cl^- channels is suggested by the widely different single-channel conductances (Kidd & Thorn, 2000) which range from 2 to 30 pS. In order to estimate the single channel conductance of CaCC in mIMCD-K2 cells both stationary and non-stationary noise analysis on whole cell currents were performed. Stationary noise analysis yielded a single channel conductance of 6.2 ± 0.8 pS and a channel density per cell of 5561 ± 311 ($n = 5$). Non-stationary noise analysis generated a similar single channel conductance of 7.1 ± 0.9 pS and a density of 4251 ± 251 ($n = 6$, n.s. *versus* stationary, unpaired Student's t test).

In conclusion, our data indicate that CaCC in mIMCD-K2 cells is a small conductance Cl^- channel whose activity is tightly coupled to changes in $[Ca^{2+}]_i$ over the normal physiological range.

Boese SH *et al.* (2000). *J Physiol* **523**, 325–338.

Kidd JF & Thorn P (2000). *Ann Rev Physiol* **62**, 493–513.

This work was supported by the NKRF

C20

Voltage-dependent and -independent effects of intracellular pH on the human CFTR Cl^- channel

J.H. Chen, Z. Cai and D.N. Sheppard

Department of Physiology, University of Bristol, Bristol BS8 1TD, UK

The cystic fibrosis transmembrane conductance regulator (CFTR) is a Cl^- channel with complex regulation. We previously demonstrated that intracellular pH has multiple effects on the activity of CFTR (Chen *et al.* 2002). To elucidate how pH modulates the activity of CFTR, we investigated the effects of voltage on the CFTR Cl^- channel at different values of intracellular pH using excised inside-out membrane patches

from C127 cells stably expressing wild-type human CFTR (for Methods, see Lansdell *et al.* 2000).

Membrane patches were bathed in symmetrical 147 mM Cl^- solutions and the bath (internal) solution contained PKA (75 nM) and ATP (1 mM) at 37 °C. To adjust the bath solution to pH 8.3 and pH 6.3, we used Tris and H_2SO_4, respectively. Data are means ± S.E.M. of *n* observations and statistical analyses were performed using Student's paired *t* test.

We began by studying the effect of voltage on the inhibition of CFTR Cl^- currents at pH 8.3. At pH 8.3, CFTR Cl^- currents were decreased by equivalent amounts at negative and positive voltages (e.g. −100 mV: pH 7.3, 100 %; pH 8.3, 75 ± 5 %; +100 mV: pH 7.3, 100 %; pH 8.3, 75 ± 4 %; $n = 4$). Consistent with these data, at pH 8.3 the open probability (P_o) of CFTR was decreased at both negative voltages (e.g. −80 mV: pH 7.3, $P_o = 0.42 \pm 0.004$; pH 8.3, $P_o = 0.32 \pm 0.01$; $n = 5$; $P < 0.01$) and positive voltages (e.g. +80 mV: pH 7.3, $P_o = 0.42 \pm 0.02$; pH 8.3, $P_o = 0.34 \pm 0.01$; $n = 5$; $P < 0.01$). However, at pH 8.3 there was a small, but significant, decrease in single-channel current amplitude (i) at negative voltages (e.g. −80 mV: pH 7.3, −1.00 ± 0.02 pA; pH 8.3, −0.92 ± 0.03 pA; $n = 5$; $P < 0.01$). This decrease in i was relieved at positive voltages (e.g. +80 mV: pH 7.3, −0.95 ± 0.03 pA; pH 8.3, −0.95 ± 0.03 pA; $n = 5$; $P = 0.48$).

Next, we studied the effect of voltage on the stimulation of CFTR Cl^- currents at pH 6.3. Voltage was without effect on i at pH 6.3 either at negative or positive voltages. Similarly, at pH 6.3 the increase of P_o was also voltage independent (e.g. −80 mV: pH 7.3, 0.43 ± 0.01; pH 6.3, 0.65 ± 0.03; $n = 6$; $P < 0.01$ and +80 mV: pH 7.3, 0.44 ± 0.02; pH 6.3, 0.64 ± 0.01; $n = 6$; $P < 0.01$).

In conclusion, our data demonstrate that pH-dependent changes in P_o are voltage independent, but that the decrease in i at pH 8.3 is voltage dependent. These data suggest that intracellular pH might modulate CFTR activity primarily by altering the function of the cytoplasmic domains of CFTR that control channel gating.

Chen JH *et al.* (2002). *J Physiol* **544.P**, 15*P*.

Lansdell KA *et al.* (2002). *J Physiol* **524**, 317–330.

This work was supported by the CF Trust and the University of Bristol.

C21

Inhibition of anion efflux through human CFTR by extracellular Cl^- is modulated by intracellular Ca^{2+} concentration

A.M. Wright, B.E. Argent and M.A. Gray

School of Cell and Molecular Bioscience, University of Newcastle Upon Tyne, NE2 4HH, UK

Cystic fibrosis transmembrane conductance regulator (CFTR) plays a central role in the secretion of a HCO_3^--rich fluid by the ductal tree of the pancreas. We have previously shown, using fast whole cell recording (WCR), that Cl^- efflux through CFTR is inhibited when extracellular Cl^- is replaced with various anions, including HCO_3^- (O'Reilly *et al.* 2000). The degree of inhibition of Cl^- efflux is not voltage dependent, nor is it related to the relative permeability of the replacement anion, suggesting that an intrapore effect is unlikely. The aim of this study was to investigate the mechanism by which Cl^- efflux through CFTR is inhibited. The experiments were performed on CHO cells stably transfected with human CFTR.

Iso-osmotic replacement of external NaCl (155.5 mM down to 6.5 mM) with mannitol in fast WCR caused a dose-dependent inhibition of inward current, in a manner identical to the effects observed following anion replacement. This indicates that a reduction in external $[Cl^-]$ alone is sufficient to produce the inhibitory effect. Comparable results were obtained using the slow WCR configuration, but the inhibition caused by reducing external $[Cl^-]$ was significantly less under these conditions over a concentration range (Student's unpaired *t*-test, $P < 0.05$). For example, when extracellular Cl^- was lowered from 155.5 mM to 116.5, 91.5 or 71.5 mM (mannitol replacement) the mean percentage inhibitions during fast WCR were 36.3 ± 3.6, 43.6 ± 8.7 and 59.1 ± 7.6, respectively (mean ± S.E.M., $n = 4$–6), compared to 12.2 ± 4.4, 7.2 ± 1.6 and 24.4 ± 2.3, respectively, during slow WCR. Overall, the dose–response curve for slow WCR is shifted to the left by ~50 mM, suggesting that loss of a cytosolic factor (in fast WCR) increases the inhibition. A reduction in internal $[Cl^-]$, from 114 down to 54 mM, did not affect the peak stimulated Cl^- current density, nor alter the subsequent inhibition of efflux by extracellular Cl^- replacement. The addition of GTP (0.2 mM) to the pipette solution during fast WCR also had no effect on the inhibition of Cl^- efflux. However, increasing the internal $[Ca^{2+}]$ from the control value of 1 nM to 100 nM during fast WCR reduced the degree of inhibition to levels comparable with slow WCR. Under these conditions, the mean percentage inhibition of the inward current was 9.3 ± 8, 23.5 ± 3.5 and 30.7 ± 5 at 116.5, 91.5 and 71.5 mM external $[Cl^-]$, respectively.

These data suggest that intracellular $[Ca^{2+}]$ can modulate the inhibitory effect of extracellular Cl^- replacement on Cl^- efflux through CFTR. In the pancreatic duct, changes in luminal $[Cl^-]$ may act as a signal that couples changes in the luminal environment to the secretory activity of CFTR.

O'Reilly *et al.* (2000). *Gastroenterology* **118**, 1187–1196.

This work was supported by the Wellcome Trust.

C22

Expression of functional voltage-gated sodium ion channels in a metastatic cell line of human breast cancer

S.P. Fraser*, J.K.J. Diss*, R.C. Coombes † and M.B.A. Djamgoz *

*Departments of *Biological Sciences and †Cancer Medicine, Imperial College London, London SW7 2AZ, UK*

We have shown previously that functional voltage-gated Na^+ channels (VGSCs) were expressed specifically in strongly metastatic rat and human prostate cancer (PCa) cell lines (Grimes *et al.* 1995; Laniado *et al.* 1997). This VGSC was tetrodotoxin (TTX) sensitive, Nav1.7 being the predominant subtype expressed (Diss *et al.* 2001). Furthermore, blocking VGSC activity in these cells suppressed a variety of cellular behaviours involved in the metsatatic cascade, such as basic and galvanotactic motility (Fraser *et al.* 1998; Djamgoz *et al.* 2001), endocytic membrane activity (Mycielska *et al.* 2001) and Matrigel invasion (Grimes *et al.* 1995; Laniado *et al.* 1997). In the present study, we have investigated whether a similar situation may exist in breast cancer (BCa) cell lines of markedly different metastatic ability.

Whole-cell patch clamp recordings were obtained from MCF-10A, MCF-7 and MDA-MB-231 cells cultured in RPMI 1640 medium with 10 % fetal bovine serum. Voltage-gated currents were activated by applying depolarizing pulses in steps of 10 mV from a holding potential of −100 mV. The basic electrophysiological observations are summarised in Table 1. In essence, an inward current was present in 29 % ($n = 56$) of the strongly

metastatic MDA-MB-231cells, but in none of the other cell lines tested. On the other hand, outward current density was inversely related to the cells' metastatic ability, such that only very small outward currents were recorded in the MDA-MB-231cells. The inward currents were blocked by TTX in a dose-dependent fashion, the IC_{50} being greater than 1 μM, i.e. the VGSC was TTX-resistant. Indeed, semi-quantitative RT-PCR analyses revealed that Nav1.5 was the predominant VGSC expressed in this cell line. The possible role of VGSC activity in metastasis was tested in Matrigel invasion experiments (Boyden chambers with chemo-attractant). These functional assays showed that pre-treating cells with 10 μM TTX reduced their invasiveness by some 40 %.

Table 1. Voltage-gated channel expression in human breast cancer cell lines of varying metastatic ability

Cell type	Metastatic potential	Voltage-activated inward (Na^+) current	Voltage-activated outward current
MCF-10A	None	None	Very large
MCF-7	None/weak	None	Medium
MDA-MB-231	Strong	Yes	Very small

In conclusion: (1) Strongly metastatic BCa cells are potentially electrically excitable and (2) VGSC activity could accelerate metastasis in BCa, as found previously for PCa cells.

Diss JKJ *et al.* (2001). *The Prostate* **48**, 165–178.
Djamgoz MBA *et al.* (2001). *J Cell Sci* **114**, 2697–2705.
Fraser SP *et al.* (1998). *J Physiol* **513P**, 131*P*.
Grimes JA *et al.* (1995). *FEBS Lett* **369**, 290–294.
Laniado ME *et al.* (1997). *Am J Pathol* **150**, 1213–1221.
Mycielska M *et al.* (2001). *J Physiol* **531P**, 81–82*P*.

This work was supported by Cancer Research UK and the Pro Cancer Research Fund.

C23

Open-channel block of the human CFTR Cl^- channel by the loop diuretic furosemide

T.S. Scott-Ward, Z. Cai and D.N. Sheppard

Department of Physiology, University of Bristol, Bristol BS8 1TD, UK

The loop diuretic furosemide is widely used to inhibit the Na^+–K^+–2Cl^- cotransporter (Haas & Forbush, 2000). However, Venglarik (1997) demonstrated that furosemide inhibits the cystic fibrosis transmembrane conductance regulator (CFTR) Cl^- channel. To investigate the mechanism of furosemide inhibition of the CFTR Cl^- channel, we used inside-out membrane patches excised from C127 cells stably expressing wild-type human CFTR (for Methods, see Lansdell *et al.* 2000). The pipette (external) solution contained 10 mM Cl^- and the bath (internal) solution contained 147 mM Cl^-, 0.3 or 1 mM ATP and 75 nM PKA at 37 °C; voltage was −50 mV. We expressed data as means ± S.E.M. of n observations and we performed statistical analyses using Student's unpaired t test.

When added to the internal solution, furosemide (100 μM) caused a flickery block of single CFTR Cl^- channels that decreased both open probability (P_o; control, 0.41 ± 0.03; furosemide (100 μM), 0.17 ± 0.05; $n = 6$), and single-channel current amplitude (i; control, −0.76 ± 0.01 pA; furosemide (100 μM), −0.63 ± 0.03 pA; $n = 6$). Block was readily reversible on washing ($n = 6$). To learn whether furosemide is an open-channel blocker of CFTR, we examined the voltage dependence of furosemide inhibition. When excised patches were bathed in symmetrical 147 mM Cl^- solutions, furosemide (100 μM) strongly inhibited CFTR Cl^- currents at negative voltages. However, channel block was completely relieved at positive voltages. Using current values in the absence and presence of furosemide, the voltage-dependent dissociation constant (K_d) for furosemide inhibition at 0 mV was calculated to be 332 ± 29 μM ($n = 5$). This voltage dependence of inhibition suggests that furosemide binds within the electric field of the membrane possibly within the channel pore. If the binding site is located within the channel pore, the passage of Cl^- ions through the channel pore would be predicted to interfere with furosemide inhibition. Consistent with this idea, when the external [Cl^-] was reduced to 10 mM, the K_d of furosemide inhibition at 0 mV decreased to 156 ± 15 μM ($n = 6$; $P < 0.01$).

These results suggest that furosemide is an open-channel blocker of the CFTR Cl^- channel. They also suggest that furosemide and Cl^- ions might compete for a common binding site.

Lansdell KA *et al.* (2000). *J Physiol* **524**, 317–330.
Haas M & Forbush III B (2000). *Ann Rev Physiol* **62**, 515–534.
Venglarik CJ (1997). *Pediatr Pulmonol Suppl* **14**, 230.

This work was supported by the CF Trust and NKRF.

PC1

Regulatory volume decrease by *in situ* human chondrocytes

P.G. Bush*, J.S. Huntley†, I.J. Brenkel†, M. Moran† and A.C. Hall*

** School of Biomed. & Clin. Lab. Sci., Hugh Robson Bldg, George Sq., Edinburgh, EH8 9XD† Orthopaedics, Queen Margaret Hospital, Dunfermline KY12 0SU, UK*

Changes to chondrocyte volume have a deleterious effect on the metabolism of the extracellular matrix of articular cartilage, possibly leading to the cartilage loss characteristic of osteoarthritis (OA; Urban *et al.* 1993). Using confocal laser scanning microscopy (CLSM) we have reported that chondrocytes from areas of degenerate tissue are larger than those from non-degenerate regions (Bush & Hall, 2003). It is possible that this cell swelling results from the inability of the cells to undergo regulatory volume decrease (RVD). Here, we have tested the RVD capacity of *in situ* human chondrocytes within non-degenerate and degenerate cartilage.

Cartilage from human tibial plateaux (with Ethical permission) was obtained at total knee replacement surgery and cultured in Dulbecco's modified Eagle's medium (280 mosmol l^{-1}). The fluorescent dye calcein was incorporated into chondrocytes (calcein-AM; 5 μM, 37 °C, 30 min). The resting volume of mid zone (MZ) chondrocytes, and their RVD capacity during a rapid (< 30 s) osmotic challenge (280 to 180 mosmol l^{-1}; 21 °C) were measured from CLSM images (Zeiss LSM 510, Axioskop, × 63 ceramic water dipping lens) using analysis software (Bitplane, Zurich). Chondrocyte volumes were reported as the percentage change compared to the value before osmotic challenge and plotted against time. Data are means ± S.E.M. (total number of joints [total number of cells]).

Paired samples of relatively non-degenerate articular cartilage (AC_{ND}, (3[21])) or degenerate articular cartilage (AC_D (3[20]); demonstrating surface fibrillation) were taken from three joints. The resting volumes of cells before hypo-osmotic challenge were larger in AC_D 792 ± 44 μm^3 compared to 671 ± 41 μm^3 for AC_{ND} ($P < 0.002$; Students' paired t test). When exposed to a hypotonic challenge, there was no difference in the extent of cell swelling,

$28 \pm 4\,\%$ and $36 \pm 3\,\%$ for AC_{ND} and AC_D, respectively ($P > 0.05$). After 20 min post-osmotic challenge, cell volume had recovered from the point of maximal swelling by $32 \pm 12\,\%$ and $30 \pm 17\,\%$ for AC_{ND} and AC_D, respectively ($P > 0.05$).

Human articular chondrocytes within degenerate cartilage (AC_D) are larger than those in non-degenerate tissue (AC_{ND}), but there was no difference in the response to the hypotonic challenge. The extent of cell swelling and the rate of volume recovery by RVD were similar. These data show that the RVD mechanism activated in response to an acute hypotonic challenge is not compromised in chondrocytes within degenerate cartilage.

Bush PG & Hall AC (2003). *Osteoarthr Cartil* **11**, 242–251.
Urban JPG *et al.* (1993). *J Cell Physiol* **154**, 262–270.

This work was supported by the Arthritis Research Campaign (H0621). We thank Mr J. Aderinto for helping with the cartilage samples.

All procedures accord with current local guidelines and the Declaration of Helsinki.

PC2

Acid secretion by surface epithelium of isolated porcine distal airways

S.K. Inglis

Tayside Institute of Child Health, University of Dundee, DD1 9SY, UK

Secretion of HCO_3^- by airway submucosal glands is essential for normal liquid and mucus secretion (Inglis *et al.* 1998). Since the liquid bathing the airway surface is fairly acidic, we have proposed that the surface epithelium may acidify HCO_3^--rich glandular fluid. We previously showed that isolated distal bronchi, containing both glandular and surface epithelium, can both acidifiy and alkalinise their lumen (Inglis *et al.* 2003). The aim of the current study was to investigate whether the acidification arises from ion transport in the surface or glandular epithelium.

Porcine distal bronchi were isolated from pigs humanely killed with an overdose of sodium pentobarbital, cannulated in a bath containing HCO_3^--buffered solution and perfused ($3\,ml\,min^{-1}$) with similar solution, in which NaCl replaced $NaHCO_3^-$. This solution was lightly buffered (buffering capacity 0.6 mM pH $unit^{-1}$) with KH_2PO_4 and NaOH to pH ~7, gassed with 100 % O_2 to eliminate dissolved CO_2 and stirred vigorously. The pH of this circulating luminal solution (10 ml) was monitored continuously. Transepithelial PD was measured using a luminal microelectrode referenced to the bathing solution, connected to an electrometer.

As previously shown (Inglis *et al.* 2003), upon perfusion through the airway lumen pH initially fell by 0.057 ± 0.009 pH units ($[H^+]$ increase $2.54 \pm 0.45\ \mu mol\ h^{-1}$ (means ± S.E.M., $n = 7$)) before stabilising. Since removing the surface epithelium removes the primary resistive barrier to passive HCO_3^- transport into the lumen, subsequent experiments were carried out in the absence of HCO_3^-. HCO_3^- removal significantly reduced the acidification (pH fell by 0.033 ± 0.007 pH units; $[H^+]$ increase $0.782 \pm 0.1\ \mu mol\ h^{-1}$ (means ± S.E.M., $n = 7$, $P < 0.05$, Student's paired t test used throughout). The acidification was further inhibited ($65.0 \pm 3.8\,\%$, $n = 5$, $P < 0.05$) by luminal bafilomycin A_1 (100 nM), a vH^+-ATPase blocker. Previous results showed that bafilomycin A_1 had similar effects in the presence of HCO_3^- (Inglis *et al.* 2003). To remove surface epithelium, a nylon brush was pushed through the airway lumen. Histological analyses revealed this successfully removed surface epithelium and left underlying glandular epithelium relatively intact (see Fig. 1). Such treatment abolished transepithelial PD (control bronchi -6.3 ± 1.7 mV; epithelium-stripped bronchi 0.1 ± 0.4 mV, $n = 5$, $P < 0.05$) and significantly reduced the acidification (control bronchi 0.022 ± 0.003 pH units; epithelium-stripped bronchi 0.009 ± 0.006 pH units, $n = 5$, $P < 0.05$).

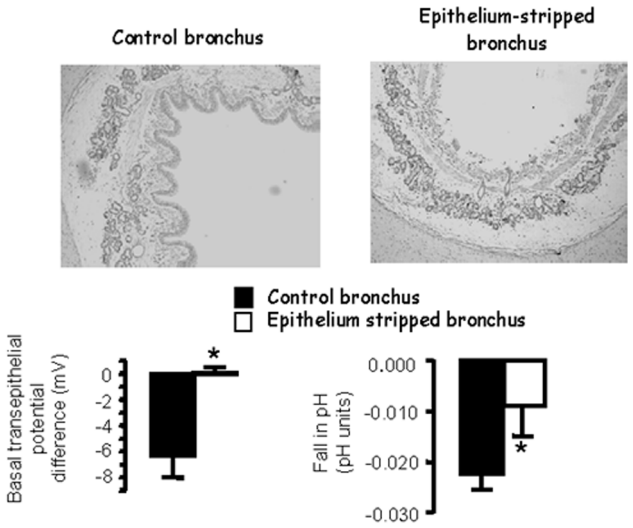

Figure 1. The effect of removing surface epithelium on acid secretion in isolated bronchi. HIstological sections show that the surface epithelium was successfully removed by brushing. Transepithelial potential difference was abolished and the fall in luminal pH was greatly reduced. Data are means ± S.E.M., $n = 5$. Asterisks indicate significant difference from control bronchi.

These data suggest that the surface epithelium has the major role in luminal acidification in intact distal bronchi, that the acidification occurs mainly through activity of vH^+-ATPase, and that the protons excreted may be generated within the epithelial cells through formation of carbonic acid from HCO_3^- and water.

Inglis SK *et al.* (1998). *Am J Physiol* **274**, L762–766.
Inglis SK *et al.* (2003). *Am J Physiol* (in the Press).

This work was supported by the Wellcome and Tenovus Trusts.

All procedures accord with current UK legislation.

PC3

Expression of KCNE1 and KCNQ1 mRNA in the proximal tubule of mouse kidney

C. Haigh*, I.D. Millar*, S.J. White†, J. Kibble‡ and L. Robson*

**Department of Biomedical Science, University of Sheffield, Western Bank, Sheffield S10 2TN, †School of Biomedical Sciences, University of Leeds, Leeds and ‡Department of Physiology & Neuroscience, St George's University, Grenada, W.I.*

In several tissues, the proteins KCNQ1 and KCNE1 (IsK) combine to form voltage-gated K^+ channels. In the proximal tubule (PT) of murine kidney, KCNE1 mediates a cell to lumen K^+ flux which may serve to counteract membrane depolarization due to electrogenic Na^+-coupled uptake of glucose or amino acids (Vallon *et al.* 2001). The aim of the present study was to demonstrate expression of KCNE1 and KCNQ1 mRNA in

isolated mouse PTs and also to determine KCNE1 protein expression in the kidney.

129/SV mice were killed by cervical dislocation and the kidneys rapidly removed for extraction of total RNA or for protein extraction. RT-PCR was performed on RNA extracted from total mouse kidney (TMK: $n = 5$ preparations) and from S1 and S2 segments of proximal tubules ($n = 5$ preparations) isolated by enzymatic digestion of cortical slices. For PCR, we used oligonucleotide primers designed against murine KCNE1 and KCNQ1 (Grahammer *et al.* 2001). The predicted size of PCR products was 355 and 421 base pairs (bp), respectively. PCR products were separated by electrophoresis on 2 % agarose gels and visualized by ethidium bromide fluorescence (302 nm).

Western blotting was performed on lysates ($n = 3$) extracted from TMK centrifuged at 15 000 *g* representing a crude membrane fraction, and then centrifuged at 50 000 *g* to obtain a cytosolic fraction. Extracted proteins were separated by 4–12 % gradient PAGE, and then electroblotted on to a nitrocellulose membrane. The membrane was incubated with an antibody against KCNE1 developed 'in house' against the C-terminal peptide of KCNE1 and visualized by standard chemiluminescent methods.

PCR products of 355 and 421 bp corresponding to KCNE1 and KCNQ1, respectively, were obtained from PT. Western blotting for KCNE1 revealed a major band at 15 kDa predominantly in the membrane fraction of the mouse kidney samples.

These experiments indicate that mRNAs for KCNQ1 along with KCNE1 are expressed in mouse proximal tubules and the protein for KCNE1 is also localized in mouse kidney membrane fractions. These results are consistent with the hypothesis that KCNQ1 and KCNE1 have a role in setting the membrane potential in the proximal tubule.

Grahammer F *et al.* (2001). *J Biol Chem* **276**, 42268–75.
Vallon V *et al.* (2001). *J Am Soc Nephrol* **12**, 2003–11.

The Wellcome Trust financed this work.

All procedures accord with current UK legislation.

PC4

Sub-cellular localisation of the Cl^- channel mediator, mCLCA1: correlation with the intracellular Cl^- channel mCLC-5

Georgina Carr*, J.A. Sayer† and N.L. Simmons*

*School of *Biosciences and †Medicine, Medical School, Framlington Place, University of Newcastle upon Tyne, Newcastle upon Tyne NE2 4HH, UK*

Mouse renal inner medullary collecting duct cells (mIMCD-3 cell-line) express several members of the CLCA protein family (including mCLCA1) that mediate Cl^- channel activity (Stewart *et al.* 2001) The voltage-dependent Cl^- channel mCLC-5 is also expressed in mIMCD-3 cells within acidic endosomes (Sayer *et al.* 2001). Here we report subcellular localisation of CLCA1 and correlate this to that of mCLC-5.

mIMCD-3 cells were transiently transfected alone or in combination with expression vectors for GFP fusion proteins for mCLCA1 (Sayer *et al.* 2000) and mCLC-5 (Sayer *et al.* 2001) (pCDNA3.1/mCLCA1CT-RFP, or pDsRed1/mCLC-5CT, Clontech), using Lipofectamine 2000 (Life Technologies). Positive transfectants were identified using a Leica confocal laser imaging microscope equipped (CLSM) with a Kr–Ar laser by their green/red fluorescence and analysed 24–48 h post-transfection. In order to identify plasma membrane in mCLCA1-GFP transfectants, cells were preincubated for 2 min at room temperature with TRITC-wheat germ agglutinin (WGA) in phosphate-buffered saline (PBS) or complete medium (Ham's F12/DMEM) at 50 mg ml^{-1}. Alternatively, in order to identify acidic endosmomes, cells were incubated with 75 nM lysotracker red (Molecular Probes) for 30 min in PBS or complete medium. Optical sections of positive transfectants were collected to allow analysis of co-localisation of mCLCA1-GFP fluorescence with plasma membrane, acidic endosomes and mCLC-5.

mCLCA1-GFP fluorescence at 24/48 h post-transfection was primarily associated with intracellular vesicular structures. A minor proportion of CLCA1-GFP fluorescence was co-localised with TRITC-WGA, confirming the presence of mCLCA1-GFP at the plasma membrane. mCLCA1-GFP fluorescence showed separation from both acidic endosomes and mCLC5-GFP, with only a minor overlap.The presence of mCLCA1 at the plasma membrane is consistent with mCLCA1 conferring Cl^- channel activity or acting as a Cl^- channel regulator. The virtual separation of mCLC-5 from mCLCA1 suggests that CLCA proteins could not compensate for loss of CLC-5 function in IMCD cells.

Sayer JA *et al.* (2000). *J Physiol* **527.P**, 44*P*.
Sayer JA *et al.* (2001). *J Physiol* **536**, 769–783.
Stewart GS *et al.* (2001). *J Membrane Biol* **180**, 49–64.

This work was supported by the NCKRF and the NKRF

PC5

Zinc stimulates the promoter activity of the divalent metal transporter (DMT1) gene in human intestinal Caco-2 cells

Jason Tennant*, Henry Bayele†, Deborah Johnson*, Nita Solanky†, Surjit Kaila Srai† and Paul Sharp*

* *Centre for Nutrition and Food Safety, School of Biomedical and Life Sciences, University of Surrey, Guildford, GU2 7XH and* † *Department of Biochemistry & Molecular Biology, Royal Free and University College London Medical School, London NW3 2PF, UK*

We have previously demonstrated that exposure of the human intestinal Caco-2 cell line to zinc stimulates iron uptake via an increase in DMT1 transporter expression (Yamaji *et al.* 2001). The cellular mechanisms involved in the up regulation of DMT1 by zinc are still unclear, though one possibility is that activation occurs via interaction with putative metal response elements (MRE) residing in the 5′ promoter region of the DMT1 gene (Lee *et al.* 1998). To test this possibility, we have investigated the effect of zinc on the activity of the DMT1 promoter using a reporter gene assay.

Caco-2 cells were seeded at a density of 6×10^3 cells cm^{-2} into 24-well plates. After 3 days cells were transfected using the $CaPO_4$ method with pGL3 plasmid (Promega, UK) that contained 1.6 kb of the DMT1 promoter cloned in front of a luciferase reporter gene. Three days following transfection, cells were exposed to zinc (100 μM) for 24 h and luciferase activity in cell lysates was measured by luminescence.

Zinc stimulation of Caco-2 cells transfected with the DMT1 promoter construct significantly increased luciferase activity compared with unstimulated cells (control 928 ± 79 a.u. *vs.* +Zn 4702 ± 348 a.u., means ± S.E.M., $n = 6$, $P < 0.0001$, Student's unpaired t test). This suggests that zinc may promote the absorption of iron by Caco-2 cell monolayers by activating a transcription factor that can interact with a specific consensus

sequence within the DMT1 promoter. The nature of the transcription factor is unknown but the zinc-inducible MTF-1 that binds to MRE sequences in several genes (Andrews, 2001) is a possible candidate. Further studies are underway in our laboratory to further identify the mechanisms involved in this response.

Andrews GK (2001). *Bimetals* **14**, 223–227.
Lee PL *et al.* (1998). *Blood Cells Mol Dis* **24**, 199–215.
Yamaji S *et al.* (2001). *FEBS Lett* **507**, 137–141.

This work was funded by BBSRC grant (90/D13400).

PC6

DMT1 protein expression in the apical membrane of human intestinal Caco-2 cells is rapidly decreased following exposure to iron

Deborah Johnson, Jason Tennant and Paul Sharp

Centre for Nutrition and Food Safety, School of Biomedical and Life Sciences, University of Surrey, Guildford GU2 7XH, UK

The transporter DMT1 mediates uptake of iron from the diet by intestinal enterocytes. Recently, we have shown that DMT1 protein expression in the plasma membrane of human intestinal Caco-2 cells is decreased by exposure to iron in a dose-dependent fashion (Sharp *et al.* 2002). Intriguingly, whole cell levels of DMT1 do not change, suggesting that the transporter may be internalised into an intracellular compartment. In this study we have investigated the time course of the iron-dependent decease in DMT1 in Caco-2 cells to determine whether changes in expression might occur within a physiologically relevant period coincident with the digestion and processing of a meal in the normal gastrointestinal tract.

Caco-2 cells were grown in 25 cm^2 flasks for 21 days. Cells were incubated with 100 μM $FeCl_3$ for up to 24 h. At the end of the experimental period, whole cell and plasma membrane proteins were isolated and utilised for Western blotting and total RNA extracted and subjected to RT-PCR for DMT1. In some experiments, membrane proteins were biotinylated prior to exposure to iron. In these studies, at the end of the incubation period, cells were lysed and the amount of biotinylated DMT1 in the cytosol determined following immunoprecipitation with DMT1 antibody, protein separation by western blotting and visualisation with streptavidin-HRP and enhanced chemiluminescence.

Plasma membrane DMT1 was significantly reduced by 4 h exposure to iron (0 h, 91.4 ± 6.7 a.u.; 4 h, 52.9 ± 11.1 a.u., means ± S.E.M., $n = 4$, $P = 0.025$, Student's unpaired t test). However, whole cell levels of DMT1 were unaltered by iron exposure. DMT1 mRNA levels isolated from control and iron-treated cells were not significantly different at this time. Interestingly, there was an increase in biotinylated DMT1 in the cytosol following exposure to iron (control 8.3 a.u., +Fe 23.7 a.u., $n = 2$). Taken together, these data suggest that the initial cellular response to elevated iron involves a decrease in apical membrane expression of DMT1, perhaps due to internalisation of the transporter into an intracellular compartment. These changes are rapid (between 1 and 4 h following exposure to iron) and could occur within the time scale for the digestion and processing of a meal.

Sharp P *et al.* (2002). *FEBS Lett* **510**, 71–76.

This work was funded by BBSRC (project grant 90/D13400).

PC7

D-Glucose does not inhibit adenosine transport in fibroblasts from *Cat2*- or *iNOS*-deficient mice

P. Casanello*† C. MacLeod‡ and L. Sobrevia*

**Cellular and Molecular Physiology Laboratory* (*CMPL*), *Department of Physiology, Faculty of Biological Sciences, †Department of Obstetrics and Gynaecology, Faculty of Medicine, University of Concepción, P.O. Box 160-C, Concepción, Chile and ‡UCSD Cancer Center, La Jolla, USA*

Expression of equilibrative nucleoside transporters 1 (ENT1, inhibited by nanomolar nitrobenzylthioinosine, NBMPR) is reduced by D-glucose, an effect associated with activation of the L-arginine/NO pathway (Parodi *et al.* 2002). We investigated whether the inhibitory effect of elevated D-glucose on adenosine transport depends on expression of cationic amino acid transporters 2 (CAT2) and the inducible NO synthase (iNOS).

Mouse embryonic fibroblasts (MEFs) from humanely killed wild-type, *Cat2*- and *iNOS*-deficient mouse (Ethics Committee approval was obtained) were cultured (24 h) in medium 199 (M199), containing 10 % newborn calf serum, 3.2 mM L-glutamine, and 5 or 25 mM D-glucose. Adenosine transport ([2,8,5-^{3}H]adenosine, 60 Ci mmol^{-1}, 0–500 μM, 2 μCi ml^{-1}, 22°C, 20 s) was measured in cells incubated (0–24 h) with M199 in the absence or presence of cytokines (10 ng ml^{-1} IL1-β + 10 ng ml^{-1} TNF-α + 20 I.U. ml^{-1} INF-γ), N^G-nitro-L-arginine methyl ester (L-NAME, 100 μM), *S*-nitroso-*N*-acetyl-L,D-penicillamine (SNAP, 10 μM), or NBMPR (1–1000 nM). CAT2 and iNOS mRNA was amplified by reverse transcriptase-polymerase chain reactions. iNOS activity was determined by L-[^{3}H]citrulline formation from L-[^{3}H]arginine (4 μCi ml^{-1}, 30 min)(Casanello & Sobrevia, 2002).

Adenosine transport in wild-type, *Cat2*–/– and *iNOS*–/– MEFs (1.2 ± 0.12, 1.1 ± 0.06 and 1.2 ± 0.2 pmol (mg protein)$^{-1}$ min^{-1}, respectively; means ± S.E.M., $n = 8$–16) was inhibited ($P < 0.05$, Student's unpaired t test) by 1 nM NBMPR (0.1 ± 0.02, 0.2 ± 0.01 and 0.2 ± 0.02 pmol (mg protein)$^{-1}$ min^{-1}, respectively). Elevated D-glucose reduced the V_{max} (12 ± 2 *vs* 43 ± 5 pmol (mg protein)$^{-1}$ min^{-1}, $P < 0.05$, $n = 12$) with non- significant changes in the apparent K_m (84 ± 12 *vs* 101 ± 24 μM) for NBMPR-sensitive adenosine transport in wild-type MEFs. Adenosine transport in *Cat2*–/– or *iNOS*–/– MEFs was unaltered ($P > 0.05$). Cytokine-activated wild-type MEFs cultured in 5 mM D-glucose reduced adenosine transport to similar values determined in 25 mM D-glucose. ENT1 mRNA level was reduced (47 ± 4 %) by 25 mM D-glucose only in wild-type MEFs. D-Glucose or cytokine effects on adenosine transport activity and expression were blocked by L-NAME, and mimicked by SNAP. These results suggest that adenosine transport via ENT1 depends on expression of CAT2 and iNOS in MEFs.

Casanello P Sobrevia L (2003). *Circ Res* **91**, 127–134.
Parodi J *et al.* (2002). *Circ Res* **90**, 570–577.

This work was supported by FONDECYT (1030781, 1030607, 1000354, 7000354) and DIUC-University of Concepción (201.084.003-1.0)–Chile, The Welcome Trust (UK) and Fulbright Commission (USA).

All procedures accord with current local guidelines.

PC8

Effects of purine receptor agonists on whole cell currents from frog isolated proximal tubule cells

J.P. Davies and L. Robson

Department of Biomedical Science, University of Sheffield, Western Bank, Sheffield S10 2TN, UK

Extracellular ATP activates P2X purinoceptors, a class of receptors that form Ca^{2+} permeable channels. A previous study has demonstrated that inhibitors of one of these, $P2X_7$, block volume regulation in frog isolated proximal tubule cells (Davies & Robson, 2002). The aim of the following study was to identify whether whole cell ATP-activated currents observed in the frog proximal cells were mediated by $P2X_7$.

Frogs were killed humanely by cervical dislocation and single proximal tubule cells were isolated from frog kidneys by enzyme digestion (Hunter, 1989). Standard patch clamp techniques were used to gain whole cell patches via the basolateral membrane. The pipette solution contained (mM): 100 NaCl, 2 $MgCl_2$, 0.5 EGTA and 10 Hepes (NaOH). The bath solution contained (mM): 100 NaCl, 0.5 $MgCl_2$, 0.5 $CaCl_2$ and 100 Hepes (NaOH). Whole cell potential was held at −100 mV and was then ramped between −100 and +20 mV. To examine agonist potency, patches were exposed to either 500 μM ATP and 500 μM 2′,3′-*O*-(4-benzoylbenzoyl)-ATP (BzATP) or 500 μM ATP and 500 μM 2-methylthio-ATP (2MeSATP). Under both circumstances the order of exposure to the agonists was altered with each patch. Data are expressed as means ± S.E.M. Statistical analysis was performed using Student's paired *t* test and significance was assumed at the 5% level.

Addition of 500 μM ATP to the extracellular surface of patches increased outward conductance (G_{out}) and inward conductance (G_{in}) by 9.55 ± 1.61 and 5.45 ± 1.00 μS cm^{-2}, respectively (n = 20). In paired patches, ATP increased G_{out}, while BzATP was without effect. The ATP-activated G_{out} was 7.11 ± 1.97 μS cm^{-2} (n = 12), while BzATP did not give a significant shift in G_{out}(0.14 ± 0.93 μS cm^{-2}). In contrast, both ATP and 2-MeSATP increased G_{out} by 11.1 ± 1.35 μS cm^{-2} and 3.64 ± 0.89 μS cm^{-2}, respectively (n = 25). The ATP-activated conductance was significantly greater than the 2-MeSATP activated conductance.

These data suggest that single proximal tubule cells isolated from frog kidney contain an ATP-activated conductance. The relative potencies of the P2X agonists ATP and BzATP suggest that the conductance is not due to $P2X_7$. The relative potencies of ATP and 2-MeSATP suggest that the activated conductance may be mediated by either $P2X_4$, $P2X_5$ or $P2X_6$. Further studies are needed to distinguish between these receptors.

Davies J & Robson L (2002). *J Physiol* **544.P**, 98*P*.

Hunter M (1989). *J Physiol* **416**, 13*P*.

This work was supported by the Wellcome Trust.

All procedures accord with current UK legislation.

PC9

cAMP-dependent regulation of basolateral glycyl-sarcosine uptake by human intestinal Caco-2 cell monolayers

F.D. Henderson*, A.D. Ayrton†, N.L. Simmons* and D.T. Thwaites*

** Department of Physiological Sciences, The Medical School, Framlington Place, Newcastle upon Tyne NE2 4HH and † GlaxoSmithKline, DMPK, The Frythe, Welwyn, Hertfordshire AL6 9AR, UK*

The activity of the proton-coupled apical peptide transporter of human intestinal cells (hPepT1) is regulated indirectly through a functional couple with the apical Na^+/H^+ exchanger NHE3 (Thwaites *et al.* 2002). In contrast, the peptide transporter present at the basolateral membrane shows a different dependence upon pH and is directly dependent upon medium Na^+ but independent of basolateral NHE1 activity (Henderson *et al.* 2002). We now report that the basolateral peptide transporter is negatively regulated by vasoactive intestinal peptide (VIP) acting via intracellular cAMP.

[^{14}C]Gly-Sar (10 μM, 0.5 μCi ml^{-1}, 30 min) uptake (37 °C) across the basolateral membrane was measured as described previously (Henderson *et al.* 2002) in Na^+-containing (137 mM NaCl) or Na^+-free (choline-Cl replacement) Krebs–Ringer solution (pH 5.5). In Na^+-containing media, basolateral [^{14}C]Gly-Sar uptake was significantly inhibited by 10 nM VIP and 10 mM forskolin from 15.73 ± 1.26 to respectively 8.44 ± 0.68 and 7.76 ± 0.57 pmol cm^{-2}. (30 min)$^{-1}$ (means ± S.E.M., n = 6, $P < 0.001$ *vs.* control, ANOVA). Ten nanomolar pituitary adenylate-cyclase activating peptide (PACAP) and 10 mM 8-Br-cAMP also inhibited basolateral [^{14}C]Gly-Sar uptake, but 10 mM dideoxyforskolin was without inhibitory effect. Additions of VIP, PACAP, forskolin and 8-Br-cAMP in combination did not inhibit basolateral [^{14}C]Gly-Sar uptake further. In Na^+-free media, basolateral [^{14}C]Gly-Sar uptake was inhibited from 19.54 ± 1.98 to 9.06 ± 0.72 pmol cm^{-2} (30 min)$^{-1}$ (n = 6, $P < 0.001$ *vs.* control), and VIP, PACAP, forskolin and 8-Br-cAMP were without effect. The kinetics of basolateral Gly-Sar uptake in Na^+-containing media are best fitted by a saturable component (K_m 5.78 ± 1.31 mM, V_{max} 5686 ± 1343 pmol cm^{-2} (30 min)$^{-1}$) and linear component of 81.8 ± 56.9 × 10^3 cm^{-1} (30 min)$^{-1}$. In the presence of forskolin (10 mM) inhibition is associated with a marked reduction of the V_{max} of the saturable component to 168 ± 27 pmol cm^{-2} (30 min)$^{-1}$. Finally, in Na^+-containing medium the inhibitory action of VIP was of high affinity (half-maximal inhibition at 27 ± 17 pM (S.E.M.)).

In conclusion VIP acting via cAMP downregulates the saturable Na^+-dependent component of dipeptide uptake at the basolateral membrane of human intestinal Caco-2 epithelial cells.

Henderson FD *et al.* (2002). *J Physiol* **539.P**, 21*P*.

Thwaites DT *et al.* (2002). *Gastroenterology* **122**, 1322–1333.

F.D.H.'s studentship was sponsored by GlaxoSmithKline.

PC10

The antimicrobial peptide hepcidin decreases iron uptake by human intestinal Caco-2 cells

Sachie Yamaji*, Bala Ramesh*, Paul Sharp† and Surjit Kaila Srai*

** Department of Biochemistry & Molecular Biology, Royal Free and University College London Medical School, London NW3 2PF and † Centre for Nutrition and Food Safety, School of Biomedical and Life Sciences, University of Surrey, Guildford GU2 7XH, UK*

Hepcidin is a 25 amino acid peptide produced in the liver whose expression is increased by iron loading and decreased in iron deficiency (Pigeon *et al.* 2001). This site of synthesis and the dramatic regulation by iron has led to the suggestion that hepcidin might be the master controller of iron metabolism, relaying information about the status of the body iron stores to the intestine and regulating absorption accordingly. The mode of action of hepcidin is still unclear. In this study we have utilised the Caco-2 cell model of human intestinal epithelial cells to investigate the possibility that hepcidin might interact directly with the epithelium.

Cells were cultured in Transwell plates for 21 days. For the final 24 h of the culture period, human synthetic hepcidin (30 μg ml^{-1}) was added to the basolateral medium. At the end of the incubation period cells were either used to measure ^{55}Fe transport across the Caco-2 cell monolayers, processed for Western blotting for the iron transport proteins DMT1 and IREG1, or used as a source of RNA to determine changes in transporter expression by Real-Time RT-PCR.

Following exposure to hepcidin, iron uptake across the apical membrane of Caco-2 cells was significantly decreased (control 453.3 ± 47.0 pmol cm^{-2} h^{-1}; +hepcidin 268.3 ± 63.8 pmol cm^{-2} h^{-1}, means ± S.E.M. $n = 6$, $P = 0.04$ Student's unpaired t test). Efflux across the basolateral membrane was unaffected by hepcidin treatment. In agreement with the transport data, the expression of the apical membrane transporter DMT1 was decreased by hepcidin treatment at both the protein and mRNA level, whereas expression of IREG1, the basolateral efflux protein, was unaffected.

Pigeon C (2001). *J Biol Chem* **276**, 7811–7819.

PC12

Intracellular pH regulation in isolated human colonic crypts

A.G. Butt

Department of Physiology, University of Otago, Dunedin, New Zealand

In the human colon the removal of HCO_3^- from the bathing medium reduces the cAMP-dependent secretory response by 60 % (Taylor *et al.* 2001). As this HCO_3^--dependent secretion is independent of Cl^- and inhibited by serosal 4,4′-diisothiocyanostilbene-2,2′-disulfonate (DIDS) it is likely that it is mediated via a basolateral $NaHCO_3$ cotransporter. Therefore, we have used measurements of intracellular pH (pH_i) to determine if a $NaHCO_3$ cotransporter is present in the secretory cells of the human colon.

All measurements used crypts isolated from colonoscopy biopsies collected from the descending and sigmoid colon. Isolated crypts were loaded with the pH-sensitive fluorescent dye 2′,7′-bis(2-carboxyethyl)-5(6)-carboxyfluoroscein (BCECF) and pH_i was measured in the basal third of the crypts at 37 °C. To characterize the pH_i regulatory mechanisms, cells were acidified with an NH_4Cl pre-pulse and the activity of pH_i regulatory mechanism quantified by the initial rate of recovery of pH_i, expressed as ΔpH units min^{-1}. All data are given as means ± S.E.M. and n = number of crypts. The experiments were approved by the Otago Ethics Committee, Dunedin, New Zealand.

In HCO_3^--free Ringer solution, pH_i recovery was dependent upon the presence of Na^+ (ΔpH units min^{-1} in presence = 0.19 ± 0.02, $n = 12$ and absence of $Na^+ = -0.022 \pm 0.007$, $n = 15$; $P < 0.05$, Student's unpaired t test). It was also inhibited in a dose-dependent manner by amiloride ($K_i = 8$ μM) with complete inhibition occurring at 0.5 mM (ΔpH units min^{-1} = −0.004 ± 0.002, $n = 4$). In the presence of HCO_3^-/CO_2, recovery of pH_i was also dependent upon Na^+ (ΔpH units min^{-1} in presence = 0.100 ± 0.013, $n = 6$ and absence of $Na^+ = -0.023 \pm 0.006$, $n = 11$; $P < 0.01$, ANOVA, Dunnett's *post* test). However, although the recovery was inhibited by 0.5 mM amiloride (ΔpH units min^{-1} 0.0215 ± 0.005, $n = 6$, $P < 0.01$, ANOVA, Dunnett's post test), there was evidence of amiloride-insensitive pH_i recovery. This amiloride-insensitive pH_i recovery was inhibited by DIDS. Following exposure to NH_4Cl and Na^+-free Ringer solution the rate of recovery of pH_i in the presence of 0.5 mM amiloride was 0.0789 ± 0.009 pH units min^{-1} ($n = 18$), whereas in the presence of amiloride plus 250 μM DIDS this was reduced to 0.0176 ± 0.005 pH units min^{-1} ($n = 9$, $P < 0.01$, unpaired Student's t test).

These data demonstrate that the dominant mechanism for regulation of pH_i in human colonic crypts under basal conditions is a Na^+/H^+ exchanger. There is also a small contribution from a HCO_3^--dependent transporter, most likely a $NaHCO_3$ cotransporter. It remains to be established whether this is stimulated by secretagogues and so contributes to the secretory response of the intact colon.

Taylor *et al* (2001). *Pflugers Arch* **442**, 256–262.

This work was funded by the University of Otago.

All procedures accord with current local guidelines and the Declaration of Helsinki.

PC14

Protein kinase C mediates the inhibitory effect of substance P on pancreatic ductal HCO_3^- secretion

P. Hegyi*, M.A. Gray and B.E. Argent

*School of Cell and Molecular Biosciences, University Medical School, Newcastle upon Tyne, NE2 4HH, UK and * First Department of Medicine, University of Szeged, Szeged, 6722, Hungary*

The regulatory pathways that stimulate pancreatic ductal HCO_3^- secretion are well described, but less is known about inhibitory pathways. Inhibitory pathways may be important in terms of limiting the hydrostatic pressure within the ducts (so preventing leakage of enzymes into the parenchyma of the gland), and in terms of switching off pancreatic secretion after a meal. Substance P (SP) inhibits secretin-stimulated HCO_3^- secretion (Ashton *et al.* 1990), and we have recently reported that SP exerts its effect by inhibiting an apical Cl^-/HCO_3^- exchanger in the duct cell (Hegyi *et al.* 2001). The purpose of this study was to identify the intracellular signalling pathway utilized by SP.

Guinea-pigs (150–250 g) were humanely killed, the pancreas was removed and small intra/interlobular ducts were isolated and

cultured overnight as previously described (Argent *et al.* 1986). The rate of HCO_3^- secretion was determined by measuring the initial rate of intracellular acidification (using BCECF) following sudden block of basolateral $NaHCO_3$ cotransporters and Na^+/H^+ exchangers with DIDS (100 μM) and amiloride (200 μM), respectively (Szalmay *et al.* 2001). The buffering capacity of duct cells was estimated and the rate of transmembrane H^+ flux, J_H, was calculated. Since H^+ and HCO_3^- will largely be derived from H_2HCO_3, we have assumed that J_H is equivalent to J_{HCO3}. All the experiments were performed in HCO_3^--buffered Ringer solution at 37 °C.

Secretin (10 nM) elevated the basal J_H about 3-fold from 2.18 ± 0.2 mM min^{-1} to 6.3 ± 1.5 mM min^{-1} ($n = 6$ ducts, $P < 0.05$, means ± S.E.M. and Student's t test). SP (20 nM) had no effect on the basal J_H, but totally inhibited the secretin-stimulated elevation of J_H ($n = 6$ ducts). This inhibitory effect of SP could be relieved by 20 nM spantide, a SP receptor antagonist ($n = 6$ ducts). Phorbol 12,13-dibutyrate (100 nM), an activator of protein kinase C (PKC), reduced the basal J_H by 38% ($n = 7$ ducts), and totally blocked secretin-stimulated J_H ($n = 6$ ducts). In addition, bisindolylmaleimide (1 μM), an inhibitor of PKC, partially relieved the inhibitory effect of SP on secretin-stimulated J_H.

Our data suggest that SP exerts its inhibitory effect on the duct cell by activating PKC, which then inhibits apical Cl^-/HCO_3^- exchange.

Argent BE *et al.* (1986). *Q J Exp Physiol* **71**, 633–648.
Ashton N *et al.* (1990). *J Physiol* **427**, 471–482.
Hegyi P *et al.* (2001). *Pediatr Pulmonol,* suppl. 22, 206.
Szalmay G *et al.* (2001). *J Physiol* **535**, 795–807.

This work was funded by The Wellcome Trust (Grant No. 022618) and the Hungarian Scientific Research Fund (Grant No. D42188).

All procedures accord with current UK legislation.

PC15

Calmodulin binding proteins and nuclear pores shape the calcium induced translocation of calmodulin in pancreatic acinar cells

Kojiro Yano, Ole H. Petersen and Alexei V. Tepikin

The Physiological Laboratory, University of Liverpool, Crown Street, Liverpool L69 3BX, UK

It has been shown in pancreatic acinar cells (Craske *et al.* 1999) that calmodulin (CaM) undergoes intracellular redistribution after application of the calcium-releasing agonists, acetylcholine (ACh) and cholecystokinin (CCK). A large cytosolic calcium transient generated by a super-maximal dose of ACh caused a rapid rise of [CaM] in apical region and a rapid drop in the basal region while the [CaM] in the nucleus rose more slowly, and lasted long after the termination of the calcium transient. Global cytosolic calcium spikes generated by 5 pM CCK caused [CaM] spikes in the apical region that resembled cytosolic calcium spikes, and [CaM] in the basal region showed the mirror image of the apical [CaM] spikes with smaller magnitude. On the other hand, [CaM] in the nucleus showed a delayed, slower and steadier increase that stabilized in about 100 s and its fluctuations were much smaller than those of [CaM] in apical or basal region.

In order to understand these behaviours of [CaM] during the agonist stimulations, we developed computational models using FEMLAB, an interactive environment for modelling mathematical problems based on a system of coupled partial differential equations. The model had one-dimensional geometry with three subdomains which represented the nucleus, apical and basal cytosolic regions. We assumed that calcium-free calmodulin (apoCaM) and calcium-bound calmodulin (CaCaM) could diffuse freely in the cytosol or in the nucleus, or bind to non-diffusible binding partners (apoCaM-binding proteins and CaCaM-binding proteins, respectively). It was also assumed that the diffusion between the cytosol and the nucleus was limited by nuclear pores whose permeability for CaM was dependent on cytosolic calcium concentration. Calcium concentration was set to be spatially uniform.

Our computational models showed (1) that a heterogeneous distribution of calmodulin binding proteins and the calcium dependence of the permeability of nuclear pores for CaM were the basis of the translocation of CaM induced by the change of cytosolic calcium, (2) a positive effect of calcium on the permeability for CaM explaining the delay in the accumulation of CaM in the nucleus which was observed experimentally, and (3) that binding proteins for apoCaM worked against the translocation by stabilizing free CaM concentration.

Our models can be used for the analysis of translocation of other calcium binding proteins with different properties (e.g. translocation from the cytosol to the plasma membrane or organellar membranes).

Craske M *et al.* (1999). *Proc Natl Acad Sci USA* **96**, 4426–4431.

PC16

Several charged residues in the extracellular domain of TASK-2 contribute to pH sensing

M.J. Morton, A. Abohamed, A. Sivaprasadarao and M. Hunter

School of Biomedical Sciences, Worsley Building, University of Leeds, Leeds LS2 9NQ, UK

TASK-2 is a member of the two-pore domain K^+ channel (K_{2P}) family and is sensitive to changes in extracellular pH; currents are maximal at alkaline pH but are progressively inhibited as the pH decreases (Reyes *et al.* 1998). TASK-2 is located principally in epithelial tissues, and is present in all nephron segments (Morton *et al.* 2002). TASK-2 has high sequence homology with TASK-4, yet lower similarity to TASK-1 and -3. In TASK-1 and -3, mutation of a charged amino acid, histidine, at position 98 abolished the pH sensitivity of this channel (Kim *et al.* 2000; Morton *et al.* 2003). However, no such homologous residue is present in TASK-2 implying a different pH sensing mechanism. pH sensing must involve titration of charged residues, and thus we have examined the involvement of charged residues in the extracellular domain of TASK-2 between the first trans-membrane segment and pore region by mutation to the neutral amino acids glutamine (Q) and asparagine (N).

Wild-type (WT) murine TASK-2 cDNA was subcloned into the bicistronic vector pIRES-CD8 (Invitrogen). Single point mutations were generated by a PCR-based mutagenesis approach and confirmed by automated fluorescence sequencing (Lark). Chinese hamster ovary (CHO) cells were transfected with either WT or mutant plasmid using Fugene transfection reagent (Roche). Twenty-four to 72 h post-transfection CHO cells expressing the CD8 antigen were positively identified by incubation with immunomagnetic particles coated with anti-CD8 antibody (Dynal) and subjected to whole-cell patch clamp analysis. Whole-cell currents were recorded in mammalian Ringer solution containing (mM): NaCl 145, KCl 5, $MgCl_2$ 1, $CaCl_2$ 2, Hepes 5, Pipes 5, titrated to between pH 5.8 and 8.8 with

KOH or HCl. Currents were normalized with respect to those at pH 8.8 and K_d values calculated with a single binding site model. Results are given as means ± S.E.M. and statistical significance tested using Student's unpaired *t* test.

The K_d for WT channels was pH 7.47 ± 0.08 ($n = 9$). The K_d values of mutant channels E28Q, K32N, K35N and K47N were all significantly lower than WT ($P < 0.05$); 7.12 ± 0.09 ($n = 9$), 7.20 ± 0.06 ($n = 9$), 7.27 ± 0.04 ($n = 14$) and 7.24 ± 0.06 ($n = 12$) respectively. The decrease in K_d implies a reduction in the pH sensitivity of the mutant channel. The K_d value for mutant channel H44N was not significantly different from WT; 7.43 ± 0.08 ($n = 11$).

The large extracellular domain of TASK-2 comprises approximately 50 amino acids, 13 of which are charged and therefore titratable by protons. Amongst these charged residues are five that are unique to TASK-2. The mutation of four of these charged residues to neutral amino acids resulted in a decrease in pH sensitivity. The exact mechanism of this reduction is unknown. The residues may themselves be titrated by protons or contribute to the effective concentration of protons at the pH sensor. In conclusion, three charged amino acids in the large extracellular domain contribute to the pH sensitivity of TASK-2.

Kim Y *et al.* (2000). *J Biol Chem* **275**, 9340–9347.
Morton MJ *et al.* (2002). *J Physiol* **544.P**, 103*P*.
Morton MJ *et al.* (2003). *Pflugers Arch* **445**, 577–583.
Reyes R *et al.* (1998). *J Biol Chem* **273**, 30863–30869.

This work was supported by the Wellcome Trust.

PC17

Effect of hypoxia on L-arginine transport in human fetal endothelium: role of protein kinase C and endothelial nitric oxide synthase

P. Casanello*†‡ D. Estay*, R. Rojas*, S. Rojas*, M. González*, J.D. Pearson‡ and L. Sobrevia*‡

**Cellular and Molecular Physiology Laboratory* (*CMPL*), *Department of Physiology, Faculty of Biological Sciences & †Department of Obstetrics and Gynaecology, Faculty of Medicine, University of Concepción, P.O. Box 160-C, Concepción, Chile and ‡Centre for Cardiovascular Biology & Medicine, King's College London, UK*

Fetal hypoxia has been associated with intrauterine growth restriction, a disease that reduces mRNA levels for human cationic amino acid transporters 1 (hCAT1) and 2B (hCAT2B), but increases eNOS mRNA level in human umbilical vein endothelial cells (HUVECs) (Casanello & Sobrevia, 2002), and activates protein kinase C (PKC, Langdown *et al.* 2001). We studied the involvement of PKC and nitric oxide (NO) in the modulation of L-arginine transport by hypoxia in HUVECs.

Cells isolated from normal pregnancies (Ethics Committee approval and informed patient consent were obtained) were cultured in medium 199 (containing 20% bovine sera, 3.2 mM L-glutamine), and exposed (24 h) to normoxia (21% O_2, 5% CO_2) or hypoxia (2% O_2, 5% CO_2, 93% N_2). L-Arginine transport (L-[2,3-^{3}H]arginine, 36.1 Ci mmol^{-1}, 7.5–1000 μM, 2 μCi ml^{-1}, 37°C, 1 min) was determined in the absence or presence (30 min to 24 h) of *S*-nitroso-*N*-acetyl-L,D-penicillamine (SNAP, 100 μM, 30 min, NO donor), calphostin C (100 nM, PKC inhibitor), 13-acetate, 12-myristate phorbol ester (PMA, 100 nM, PKC activator) or N^G-nitro-L-arginine methyl ester (L-NAME, 100 μM, eNOS inhibitor). hCAT1, hCAT2B and eNOS mRNAs were amplified by reverse transcriptase-polymerase chain reactions. Gene expression was also assessed on cDNA microarrays (Clontech). eNOS activity was determined by L-[^{3}H]citrulline formation from L-[^{3}H]arginine (4 μCi ml^{-1}, 30 min), and eNOS protein was detected by Western blot.

Hypoxia reduced the V_{max} for L-arginine transport (2.8 ± 0.2 *vs.* 5.1 ± 0.3 pmol (μg protein)$^{-1}$ min^{-1}, $n = 8$, $P < 0.05$, means ± S.E.M., Student's unpaired *t* test), with no significant changes in the apparent K_m (normoxia = 149 ± 15 μM, hypoxia = 125 ± 12 μM). Hypoxia reduced the hCAT-1 (50 ± 0.2%) and hCAT-2B (52 ± 0.2%) mRNA levels, but increased eNOS mRNA (46 ± 2%) and protein (1.4-fold) levels. L-Citrulline synthesis was reduced (55 ± 4%) in hypoxia. Hypoxia-induced inhibition of L-arginine transport was reversed by SNAP or calphostin C. Hypoxia increased PKCα/βII activity (2.7-fold) and PKCα gene expression (12-fold).

In summary, hypoxia-induced inhibition of the L-arginine/NO pathway could be due to reduced hCAT-1 and hCAT-2B transporter expression, an effect that may involve PKC and NO.

Casanello P & Sobrevia L, (2002). *Circ Res* **91**, 127–134.
Langdown ML *et al.* (2001). *J Endocrinol* **169**, 11–22.

This work was supported by FONDECYT (1030607, 1030781, 1000354 & 7000354), DIUC-University of Concepción (201.084.003-1.0) (Chile) and The Wellcome Trust (UK).

All procedures accord with current local guidelines and the Declaration of Helsinki.

PC18

Regulation of System A transporter 2 (SAT2) by ceramide in rat skeletal muscle cells

R. Hyde, E. Hajduch, D. Powell, P.M. Taylor and H.S. Hundal

Faculty of Life Sciences, University of Dundee DD1 5EH, UK

The SAT2 System A transporter is one of the most highly regulated Na^+-coupled transport mechanisms for small neutral amino acids (AAs) in mammalian cells and hence one most likely to have an active influence on cellular AA metabolism (Broer, 2002). The transporter is regulated at multiple levels and by many factors, including hormonal and nutritional stimuli that can modulate both its subcellular distribution and cellular expression (Hyde *et al.* 2001, 2002), and by changes in pH and electrochemical gradients that can alter transporter activity at the plasma membrane (Chaudhry *et al.* 2002). The sphingolipid ceramide (Cer) has been implicated in the pathogenesis of insulin resistance and apoptosis, because of its widely accepted role in tumour necrosis factor α signalling (Mathias *et al.* 1998). Since ceramide antagonises insulin action, we sought to determine whether it affects SAT2 function in L6 muscle cells, which is known to be regulated by insulin.

Cer induced a time- and dose-dependent decrease in System A activity, with maximal (~70%) reduction after 2 h of treatment with 100 μM Cer, whereas an inactive Cer analogue had no effect. This response was associated with a decrease in SAT2 protein in the plasma membrane, although no reduction in total cellular SAT2 content was observed. Protein synthesis and the uptake of leucine and glucose were largely unaffected by Cer, but significant changes in the intracellular AA profile for both System A and non-System A substrates was observed. Anabolic stimuli such as insulin and leucine stimulated System A activity by up to 80% following a 30 min and 3 h incubation, respectively. System A transport was also enhanced (~2-fold) upon depriving cells of AAs for 4 h. The responses to both insulin and leucine were lost

upon preincubation of L6 cells with Cer, whereas the increase in System A activity in response to AA withdrawal was unaffected.

Our results indicate that Cer suppresses transport of AAs via System A by promoting internalisation of SAT2 transporters at the plasma membrane and by desensitising the carrier to the effects of various stimuli. Since Cer levels are elevated in muscle during insulin resistance, the effects of the lipid on SAT2 may have clinical importance in Type II diabetes. Also, since System A is upregulated during cellular proliferation, the effects of pro-apoptotic compounds, such as Cer, on SAT2 may also have a role in regulated cell death.

Broer S (2002). *Pflugers Arch* **444**, 457–466.
Chaudhry FA *et al.* (2002). *J Neurosci* **22**, 62–72.
Hyde R *et al.* (2001). *Biochem J* **355**, 563–568.
Hyde R *et al.* (2002). *J Biol Chem* **277**, 13628–13634.
Mathias S *et al.* (1998). *Biochem J* **335**, 465–480.

This work was supported by the BBSRC, MRC and Diabetes UK.

PC19

The role of different types of Cl^- channels in MDCK cyst development and growth

H. Li and D.N. Sheppard

Department of Physiology, University of Bristol, Bristol BS8 1TD, UK

Polycystic kidney disease is characterised by the massive enlargement of fluid-filled epithelial cysts that disrupt kidney function. Hanaoka *et al.* (1996) demonstrated that the cystic fibrosis transmembrane conductance regulator (CFTR) Cl^- channel plays a key role in fluid accumulation within the lumen of some, but not all, cysts from patients with polycystic kidney disease. This suggests that other types of Cl^- channels might play an important role in cyst development and enlargement.

Using MDCK type I cells that express CFTR, we previously demonstrated that CFTR-driven fluid secretion increases the size of MDCK cysts (Li & Sheppard, 2002). In this study, we investigated the role of Ca^{2+}-activated and volume-sensitive Cl^- channels in cyst formation and growth. We began by assessing the function of Ca^{2+}-activated and volume-sensitive Cl^- channels in MDCK cells using the iodide efflux assay (for Methods, see Lansdell *et al.* 1998). To stimulate Ca^{2+}-activated and volume-sensitive Cl^- channels, we used ionomycin (1 μM) and a 50% hypotonic solution, respectively; to activate CFTR Cl^- channels, we used forskolin (10 μM). In type I MDCK cells, forskolin, ionomycin and hypotonicity all stimulated an efflux of iodide and the magnitude of iodide efflux decreased in the rank order: hypotonicity (82 ± 9 nmol min^{-1}) $\gg$ ionomycin (18 ± 2 nmol min^{-1}) = forskolin (14 ± 3 nmol min^{-1}; means ± S.E.M.; $n = 6$ for all values). In contrast, in type II MDCK cells that lack CFTR, only hypotonicity stimulated an efflux of iodide. However, the magnitude of the response was drastically smaller than that stimulated by hypotonicity in type I MDCK cells (10 ± 1 nmol min^{-1}; $n = 6$).

For cyst growth studies, we used cysts grown either in collagen gels or culture dishes for 6 days. Type I MDCK cysts formed using both substrates. However, type II MDCK cysts only formed in culture dishes. In the absence of drugs, a few large type I cysts with well-defined walls formed in culture dishes. However, many small type II cysts with poorly defined walls formed in culture dishes in the absence of drugs. In collagen gels, forskolin (10 μM) and ionomycin (1 μM) stimulated the formation and growth of type I MDCK cysts, but were without effect on type II MDCK cysts. The number and size of cysts grown in the presence of ionomycin (1 μM) were significantly smaller than those grown in the presence of forskolin (10 μM; $P < 0.01$; Student's unpaired t test). A 50% hypotonic solution stimulated the growth of both type I and type II MDCK cysts. Interestingly, cysts grown in the presence of a 50% hypotonic solution developed into a solid mass of cells after 2–4 days. We interpret these data to suggest that the CFTR Cl^- channel plays a dominant role in MDCK cyst formation and growth.

Hanaoka K *et al.* (1996). *Am J Physiol* **270**, C389–399.
Lansdell KA *et al.* (1998). *J Physiol* **512**, 751–764.
Li H & Sheppard DN (2002). *J Physiol* **544.P**, 87*P*.

This work was supported by the NKRF.

PC21

Isolation and functional characterisation of rat PAT2 (proton-coupled amino-acid transporter 2)

D.J. Kennedy*, Z. Chen†, V. Ganapathy† and D.T. Thwaites*

**School of Cell & Molecular Biosciences, The Medical School, Framlington Place, Newcastle upon Tyne, NE2 4HH, UK and †Department of Biochemistry and Molecular Biology, Medical College of Georgia, GA 30912, USA*

The H^+-coupled amino acid transporter PAT1 has been cloned from rat (Sagné *et al.* 2001), mouse (Boll *et al.* 2002) and human (Chen *et al.* 2003). Recently, a related transporter (PAT2) was cloned from mouse and characterised functionally following expression in *Xenopus laevis* oocytes (Boll *et al.* 2002). Here we report the cloning and functional characterisation of rat PAT2.

A rat lung cDNA library was screened using a probe designed using the mouse PAT2 cDNA sequence (Boll *et al.* 2002). *X. laevis* were killed humanely and oocytes removed for expression studies. [^{3}H]Amino acid (proline, alanine, glycine, MeAIB, leucine and lysine, all 100 μM, 5 μCi ml^{-1}) uptake (23 °C, 40 min, pH 5.0–7.4) was determined both in the presence and absence of extracellular Na^+ in *X. laevis* oocytes 3 days after injection with 50 ng rat PAT2 cRNA.

A full-length 2396 bp cDNA (including polyA tail) was isolated from a rat lung cDNA library. The cDNA encodes for a transporter protein (rat PAT2), 481 amino acids in length. At the amino acid level rat PAT2 has 93% identity with mouse PAT2 (Boll *et al.* 2002) and 75% (over amino acids 52–477) with rat PAT1 (LYAAT-1) (Sagné *et al.* 2001). Proline uptake (pH 5.0–7.4) in rat PAT2 expressing *X. laevis* oocytes was greater than that in water-injected controls ($P < 0.0001$, ANOVA), uptake being pH dependent and significantly larger ($P < 0.001$) at pH 5.5 (71.67 ± 6.62 pmol oocyte^{-1} (40 min)$^{-1}$ (20); mean ± S.E.M. (n)) than at pH 7.4 (35.25 ± 2.21 pmol oocyte^{-1} (40 min)$^{-1}$ (19)). Uptake was Na^+ independent at both pH 5.5 and 7.4 ($P > 0.05$, Na^+ *versus* Na^+-free conditions). Compared to PAT1, rat PAT2 is a high affinity transporter, K_m proline of 0.20 ± 0.04 mM. Measurement of uptake of a number of radiolabelled amino acids suggests that glycine, alanine and MeAIB are also substrates for rat PAT2 whereas leucine and lysine are not.

In conclusion, rat PAT2 was cloned from a rat lung cDNA library and functions as a high affinity pH-dependent, H^+-coupled, Na^+-independent amino acid transporter. The physiological role of this transporter requires further investigation.

Boll M *et al* (2002). *J Biol Chem* **277**, 22966–22973.
Chen Z *et al* (2003). *J Physiol* **546**, 349–361.

Sagné C *et al* (2001). *Proc Natl Acad Sci U S A* **98**, 7206–7211.

This work was supported by the MRC (G9801704), BBSRC (13/D17277) and NIH (HL64196 & AI49849).

All procedures accord with current local guidelines.